


## RESEARCH ARTICLE OPEN ACCESS

# Minimally Invasive Approaches to the High-Resolution Mapping of Colluvial Deposits at the Battlefield of Waterloo: Implications for Archaeological Practice

Duncan Williams<sup>1,2,3</sup>  | Kate Welham<sup>1</sup> | Stuart Eve<sup>1</sup> | Philippe De Smedt<sup>2,3</sup>

<sup>1</sup>Department of Archaeology & Anthropology, Bournemouth University, Bournemouth, UK | <sup>2</sup>Department of Environment, Faculty of Bioscience Engineering, Ghent University, Ghent, Belgium | <sup>3</sup>Department of Archaeology, Faculty of Arts and Philosophy, Ghent University, Ghent, Belgium

**Correspondence:** Duncan Williams ([dwilliams1@bournemouth.ac.uk](mailto:dwilliams1@bournemouth.ac.uk))

**Received:** 30 January 2024 | **Revised:** 1 October 2024 | **Accepted:** 11 February 2025

**Scientific Editor:** Rolfe Mandel

**Funding:** This work was supported in part by funding from the Social Sciences and Humanities Research Council (Canada), Waterloo Uncovered (United Kingdom), Bournemouth University, and the Gray-Milne Bursary (British Geophysical Association).

**Keywords:** battlefield archaeology | colluvium | near-surface geophysics | remote sensing | soil erosion

## ABSTRACT

Soil erosion poses a considerable threat to ecosystem services around the world. Among these, it is extremely problematic for archaeological sites, particularly in arable landscapes where accelerated soil degradation has been widely observed. Conversely, some archaeological deposits may obtain a certain level of protection when they are covered by eroded material, thereby lessening the impacts of phenomena such as plow damage or bioturbation. As a result, detailed knowledge of the extent of colluvial deposition is of great value to site management and the development of appropriate methodological strategies. This is particularly true of battlefield sites, where the integrity of artifacts in the topsoil is of great importance and conventional metal detection (with its shallow depth of exploration) is relied upon as the primary method of investigation. Using the Napoleonic battlefield of Waterloo in Belgium as a case study, this paper explores how different noninvasive datasets can be combined with ancillary data and a limited sampling scheme to map colluvial deposits in high resolution and at a large scale. Combining remote sensing, geophysical, and invasive sampling datasets that target related phenomena across spatial scales allows for overcoming some of their respective limitations and derives a better understanding of the extent of colluvial deposition.

## 1 | Introduction

Soil erosion is the process of particle detachment and movement, primarily by the action of wind, water, and tillage (Pennock 2019), while colluvium is the sedimentary product that results from Newtonian transport of weathered soil, sediment, and rock.<sup>1</sup> A recent United Nations report notes considerable acceleration in global soil erosion (FAO 2019). It is universally agreed that this is a product of anthropogenic influence (Ahmed et al. 2019; Pennock 2019), with devegetation and intensive agriculture being two particularly important

factors (French 2016). Indeed, long-term archives of colluvial deposits have demonstrated increased erosion in the recent past (Kappler et al. 2018).

Alongside threats to other ecosystem services (such as food security and water quality) (Pennock 2019), soil erosion has been cited as a critical threat to global archaeological heritage. While coastal erosion heavily linked to climate change has been a prominent focus (Dawson et al. 2020), the impact of other forms of erosion in arable landscapes has also been extensively acknowledged (Meylemans et al. 2014). Indeed, nearly two

This is an open access article under the terms of the [Creative Commons Attribution](https://creativecommons.org/licenses/by/4.0/) License, which permits use, distribution and reproduction in any medium, provided the original work is properly cited.

© 2025 The Author(s). *Geoarchaeology* published by Wiley Periodicals LLC.

decades ago, plow-induced soil erosion was noted as being the greatest threat to archaeological sites around the world (Wilkinson et al. 2006).

Soil erosion and the postdepositional movement of artifacts, which may be entrained in colluvial deposits (French 2016), is particularly problematic for archaeological research which relies on the interpretation of spatial distributions of surface or near-surface finds. One such area is battlefield archaeology, where the major focus is on the analysis of spatial patterning of conflict-related items recovered from the plowzone or topsoil (Banks 2020). Surveys are undertaken using conventional metal detectors that typically have a maximum depth of exploration of approximately 30 cm (Connor and Scott 1998, 79). Thus, objects that are buried beneath even a relatively shallow layer of colluvium may be undetectable. This is also problematic for other forms of archaeological prospection (e.g., test pitting) and has been a frequent challenge for archaeologists working in complex geomorphological environments (particularly fluvial and alluvial) (e.g., Weston 2001; Layzell and Mandel 2019; Crabb et al. 2022).

While erosion can degrade archaeological features and transport objects from their depositional context, it also has the potential to seal other deposits in situ, possibly affording them some level of protection from plow damage, bioturbation, and so on. In both cases, knowledge about the existence and extent of colluvial deposits is beneficial to the understanding and management of archaeological landscapes. Furthermore, archaeologists have long recognized that colluvial deposits are themselves excellent archives of human land use and are thus important targets for research investigating long-term human–environmental interactions (e.g., Vanwalleghem et al. 2006; Froehlicher et al. 2016; Henkner et al. 2018). This paper will examine methods for characterizing colluvial deposits at the detailed scale required for archaeological purposes. Thus, the focus is not on predicting/modeling future erosion or the quantitative characterization of soil loss (which has been extensively studied by other researchers [Boardman and Poesen 2006]) but rather the characterization of existing colluvial deposits and their relation to the archaeological record. The aims of the study are as follows:

- Describe the mechanisms of soil erosion operating in the study area (battlefield of Waterloo, Belgium).
- Characterize the impact of soil erosion and colluvial accumulation on the archaeological record of the battle.
- Consider the range of methods available for recording lateral and vertical extents of colluvial deposits, with a particular focus on noninvasive datasets (remote sensing, geophysics) and targeted minimally invasive sampling.
- Develop an integrated workflow for mapping erosion and colluvial deposits at multiple scales.

## 2 | Background: Mechanisms of Soil Erosion and Research Approaches

Water is the dominant agent of erosion in temperate climates and the main mechanism responsible for soil erosion in the case

study considered herein (Verstraeten et al. 2006). Raindrop impact causes initial soil detachment, along with overland flow (Pennock 2019). When the infiltration capacity of the soil is reached, surface flow occurs, and detached particles are transported (sheet erosion). As the water flows, it forms small incisions (rills), wherein the velocity increases. This starts the process of channelized erosion, which begins as rill erosion but can reach a greater extreme in the form of gully erosion.

Detachment and transport are determined by the resistance of soil particles to hydraulic flow. Conversely, when the flow of particles in motion decreases past a critical point, deposition occurs. This is primarily determined by slope steepness (which influences runoff velocity); topography is thus the primary factor influencing erosion potential. Erosion can occur in any location that has greater than 2° of slope (French 2016, 157).

The soil type has an impact, as texture (particle size) determines the mode by which eroded materials are transported. Clay particles resist detachment because of the high cohesion between them, while medium to larger sand particles resist transport because of their large size. Grain sizes of approximately 0.5 mm (coarse silt to fine sand) are the most susceptible to erosion (French 2016).

Vegetation cover also has a great impact, beginning with the interception and slowing of raindrops, increasing infiltration rate and soil resistance through root action, and blocking overland flow. The amount of cover is directly related to the degree of soil loss, with the type of cover also playing a role (e.g., greater resistance to erosion moving from cropland to grassland to forest) (French 2016).

Lastly, land use has an important influence and is closely linked to vegetation cover. It has also been demonstrated that tillage operations are responsible for their own form of erosion, causing downslope movement of soil primarily due to gravity. This increases exponentially with the depth of plowing and tillage speed. Other factors, such as tillage direction and implement type, also have an important influence (Van Oost et al. 2006). This mechanism differs significantly from water erosion; it does not result in net soil loss at the field scale but can transport particles to positions more susceptible to further movement via water erosion (Pennock 2019, 31–33, 42–44).

Much of the research dealing with soil erosion has focused on developing models for assessing future erosion risk and measuring and predicting soil loss (Brazier 2013). Foremost among these is the Universal Soil Loss Equation (USLE) (Wischmeier and Smith 1978) and its derivatives, which is a widely-used empirical determination of the contribution of various factors (rainfall/run-off, soil properties, slope, landcover, and management practices) to overall soil erosion. The model has also been used in archaeological contexts to examine how land use has impacted soil erosion in the past (Hill 2004; Brandolini et al. 2023).

The identification of existing colluvial deposits, especially those that are not particularly recent, has received less attention. They are typically mapped as part of regional soil surveys (undertaken with systematic field sampling), but these are relatively coarse and usually designed to be mapped at a scale of approximately

1:20,000. When higher-resolution data is sought, researchers may undertake their own sampling schemes (e.g., French et al. 2007), although this can be quite time-intensive. Another limitation of regional soil surveys is that they tend to be legacy data (typically undertaken around the mid-20th century) and perhaps not adequately representative of dynamic processes such as soil erosion.

To mitigate these challenges, researchers have relied on a variety of noninvasive observation methods for mapping soil erosion. Since topography is one of the foremost determinants of soil properties and has a critical role in soil erosion and accumulation (Schaeztl 2013), terrain derivatives obtained from elevation models constitute one of the most important and widely used predictors of colluvial deposits (Zádorová et al. 2014; Penížek et al. 2016; Đomlija et al. 2019). The widespread availability of high-resolution elevation models from LiDAR surveys has greatly enabled such work.

Other forms of remote sensing have also been used to identify colluvial deposits. Most applications focus on the use of passive optical remote sensors operating in the visible and near-infrared range. The manual interpretation of air photos, which revolutionized conventional soil survey (Ahrens 2008), is an example of such an approach and has long been used for mapping erosional features (Hills 1950; Ray 1960), including for archaeological purposes (French et al. 2007). It continues to be an important method for detailed mapping of erosion, given the high resolution of most images, and also allows for the analyses of change over time if appropriate images from different periods are available (Jenčo et al. 2020; Netopil et al. 2022).

Recently, there has been a focus on the integration of multi- and hyper-spectral optical remote sensing data for a variety of soil mapping applications (Boettinger et al. 2008). Hereby, environmental covariates (vegetation, land use, etc.) influencing soil patterns are identified based on their spectral signatures. A common application has been the characterization of soil texture using a variety of band ratios or indices with classification aided by machine learning techniques and analysis of field samples (e.g., Liao et al. 2013; Gholizadeh et al. 2018; Vaudour et al. 2019). The use of remote sensing indices for geoarchaeological modeling in alluvial environments characterized by deeply buried deposits has also been demonstrated by Crabb et al. (2022). Similar methods have also been used to characterize soil erosion with optical remote sensing data (Žižala et al. 2019). Soil mapping with remote sensing has been particularly enabled by free and open access to data from global missions such as Landsat and Sentinel platforms and, more recently, access to large databases of cloud-hosted images and processing libraries such as Google Earth Engine (Gorelick et al. 2017).

Geophysical instruments, which measure variations in (primarily electromagnetic) physical properties that can be linked to soil properties (e.g., texture), have also been incorporated into soil mapping approaches and have been particularly effective at producing high-resolution maps of soil variability at the field scale (Brogi et al. 2021). Crucially, geophysical methods offer a means of balancing the limitations of scale that characterize point measurement (difficulty capturing heterogeneity) and remote sensing (coarse resolution and low depth penetration) datasets

(Garré et al. 2023). In this regard, they could similarly be of use in soil erosion studies that struggle to bridge the gap between field observations and regional modeling based on plot experiments (Boardman 1998). They have, however, rarely been used explicitly to map colluvial deposits and erosional features,<sup>2</sup> despite being very adept at measuring important variables related to soil erodibility (such as moisture and texture).

The following sections will compare the information derived from these different methods—manual sampling at point measurements, terrain modeling, remote sensing, and geophysical survey—using select locations at the battlefield of Waterloo in Belgium as a case study. Each method has benefits and drawbacks related to the sample support (Goovaerts 2016), sensitivity, and cost associated. Combining different data sources allows for a more comprehensive understanding of depositional sequences than a single method affords.

### 3 | Case Study: Battlefield of Waterloo, Belgium

The Battle of Waterloo (June 18, 1815) famously saw the defeat of Napoleon Bonaparte by a European alliance commanded by the Duke of Wellington and Marshall Gerhard Von Blücher. It took place on the outskirts of several small villages approximately 15 km south of Brussels in Belgium (Figure 1). The present landscape is primarily used for agricultural purposes, as it was at the time of the battle. Since 2015, archaeological research has been ongoing through a project initiated by Waterloo Uncovered (a British charity combining archaeological research with veteran/serving personnel care and recovery [Evans et al. 2019]). A series of campaigns focusing on a variety of significant nodes of interest across the battlefield landscape have been undertaken (Waterloo Uncovered 2015; Bosquet et al. 2016; Eve and Pollard 2020).

The site is situated in the periglacial Late Pleistocene loess belt of northwestern Europe, part of which runs through central Belgium (Haesaerts et al. 2016; Lehmkuhl et al. 2021). Beneath the loess cover, there is a sandy Tertiary substrate dating to the Middle Eocene (ca. 50 Ma) and originating from a series of marine transgressions (Laga et al. 2002; Houthuys 2011). Soil surveys were undertaken in the 1950s and 1960s (Louis 1958, 1973), involving boreholes excavated to a depth of 125 cm at regular intervals of 75 m. These have shown that the thickness of the loess cover is quite variable due to the undulating nature of the topography, which is composed of a series of ridges separated by intervening valleys (with maximum elevation differences of ca. 40 m). On the plateaus, the loess cover can be several meters thick, while the Tertiary substrate is present on the surface in steeply sloped areas due to erosion of the Quaternary cover. Colluvial deposits are present in concavities and at the base of slopes, where the eroded loess cover has been redeposited (Louis 1973, 11–12). Approximately 85% of mapped soils in the study area are noted as being silty in texture, with the remainder either sandy or silty-sandy in strongly eroded areas (Service public de Wallonie 2005).

The typical soil type in the study area is a Luvisol (Dondeyne et al. 2014), formed under mixed forest in the postglacial period (Louis 1973, 26–28). These soils feature a clay-enriched



**FIGURE 1** | Location of study area. The highlighted parcel (Area A) is considered in additional detail.

(illuviated) B-horizon beneath a decalcified, clay-poor (eluviated) A-horizon caused by downward transport (leaching) of clay particles by rainwater. This textural B-horizon sits atop the unaltered loess parent material (C-horizon). After deforestation, the original A-horizon was removed by erosion in most areas (except those with slopes of less than  $1^\circ$ ) and replaced with an anthropogenic plowzone (Ap horizon). Colluvial deposits are typically silty with a uniform texture similar to the upslope deposits from which they derived (Louis 1973, 20–21). Extent and thickness are variable and determined by the slope character and timing of deforestation. B-horizons have not formed in colluvial deposits; instead, the Ap horizon sits directly atop the C-horizon (which may itself cover another series of buried horizons) (Louis 1973, 31).

The Belgian loess belt is highly susceptible to soil erosion, with water and tillage erosion being the primary mechanisms (Verstraeten et al. 2006, 389–400; Rommens et al. 2007), as has been observed in the study area (Figure 2). Erosion has been associated with long-term cultivation in the study area and is not solely a recent phenomenon. The time of deforestation is uncertain but based on the late 18th-century Ferraris map (Vervust 2016), the study area was largely devoid of trees by the time of the Battle of Waterloo. Net soil loss for the central Belgian loess belt has been estimated at approximately 26 tons per hectare per year, which equates to a soil profile lowering of 1.73 mm per year for a typical topsoil (Meylemans and Poesen 2014). This occurs primarily through rill and gully erosion, with sheet erosion estimated to represent about 10% of soil loss in the loess belt (Verstraeten et al. 2006, 398). Ephemeral gully erosion is thought

to be the dominant mechanism, accounting for roughly 50% of net loss (Vandaele et al. 1996; Nachtergaele et al. 2002).

Whereas water erosion has been the dominant historical mechanism of soil loss, tillage erosion has increased in significance since the introduction of mechanized agriculture (Van Oost et al. 2006; Verstraeten et al. 2006, 400). Since the 1950s, it has been the dominant process responsible for landscape alteration in central Belgium (Verstraeten et al. 2006, 400). Archaeological excavations have demonstrated that significant soil erosion has occurred in certain areas since the time of the battle, with an accumulation of  $> 1$  m in some areas (Figure 3).

Throughout the following sections, reference will be made to a ca. 14 ha subset of the larger study area located in the northwest of the site (Area A, Figure 1). At present, it is entirely used for agricultural purposes and is characterized by considerable homogeneity in soil properties, with the entire area classified as silty and well-draining.

## 4 | Methods

To assess high-level erosion risk in the study area, we consider factors outlined in the USLE, which is specifically formulated for quantifying soil loss by water erosion. Due to the small size of the study area, the effect of rainfall erosivity is assumed to be constant. Land use and support practices can also be treated as fixed variables because agricultural practices (partly governed by legislative policies) are consistent across the area, and it has



**FIGURE 2** | Example of active rill erosion in the study area.

been largely deforested since the time of interest (i.e., 1815). If the objective was to explain variable inter- or intra-field erosion rates on a yearly or seasonal basis, these factors would have to be considered; however, because the focus is on long-term depositional processes, this small-scale variability can be ignored. While soil texture is also largely homogenous, the influence of slope position on depth to Tertiary sands (Louis 1958) links textural variability closely to topography. This makes topography a key factor for examining long-term erosion susceptibility.

One of the limitations of the USLE for the present exercise is that it does not indicate areas of likely deposition (i.e., of colluvium) (Van Oost et al. 2000, 578). To address this, an approach to extract topographic landform elements is required. Here, the interest is in extracting footslope and toeslope areas

where colluvial deposition is most likely (Schaetzl 2013) (Figure 4). The geomorphons method, based on the classification of landforms from a terrain model using ternary pattern recognition of elevation differences and line-of-sight (Jasiewicz and Stepinski 2013), was used to achieve this. Landform elements are then further reduced to three categories: accumulative/depositional zones (made up of pits, valleys, footslopes, and hollows), erosive zones (peaks, ridges, shoulders, spurs, steep slopes), and stable zones (flat areas, gentle slopes). Important parameters that influence the result of the geomorphon classification are the lookup distance and flatness threshold. The former defines the search distance for each cell and, in practice, determines the largest recognizable landform element (here, 25 m). The latter provides the decision threshold at which a cell is classified as being equal in elevation to the focal cell. Here, a value of  $2^\circ$  is used, following the slope

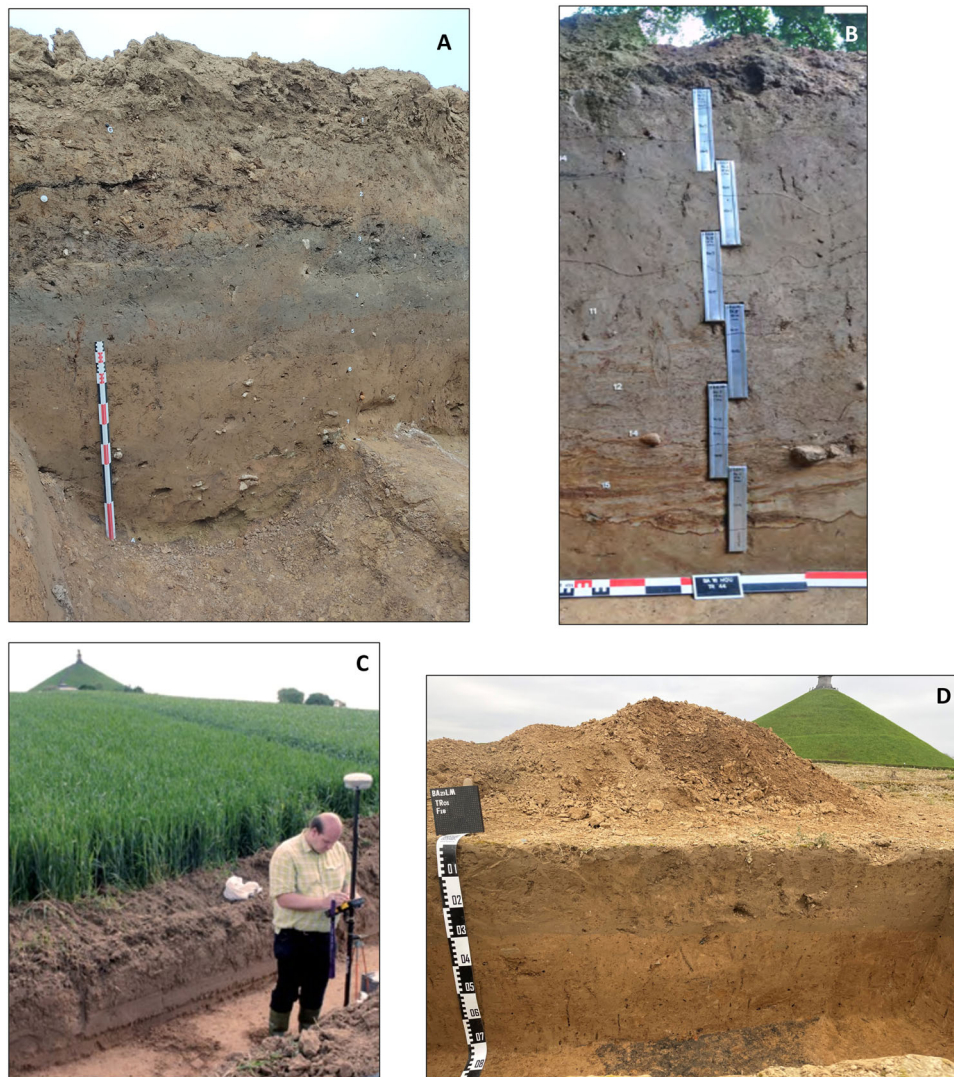


**FIGURE 3** | Examples of colluvial deposits covering archaeological features of interest. (A) quarry pit open at the time of the battle; (B) covered way near Hougoumont farm; (C) trench near the current visitor parking lot where an isolated burial was discovered (reproduced with permission, Bosquet et al. 2015); (D) remains of a forge near the Lion Mound monument.

threshold noted above. The terrain model used is a LiDAR data set collected in 2013–2014 with a measurement density averaging 0.8 pulses/m<sup>2</sup> (Service public de Wallonie 2015).

The geomorphons method generates a risk/likelihood of erosion model but does not directly identify and characterize existing colluvial deposits. For this, a contrast must exist, operating from the assumption that colluvial deposits possess measurable physical properties that can differentiate them from other (background) deposits. These differing properties (e.g., texture or organic matter content) are also likely to affect vegetation growth (Groß et al. 2023). To explore this, several remote sensing products are assessed. First, a range of high-resolution orthophoto scenes are considered. Colluvial deposits and eroded areas can be identified in certain areas of the images through visible contrasts in brightness, color, and texture.

These contrasts are, however, inconsistent across various images, depending on the seasonal and land-use conditions (especially crop type and phenological stage) at the time of

image capture. This problem has previously been recognized by researchers attempting to delineate long-term landscape features. A proposed solution has been to use multi-temporal image composites (Orengo and Petrie 2017). For this, Google Earth Engine was used to produce Landsat-8 (L8) and Sentinel-2 (S2) optical remote sensing image composites using images up to September 15, 2023. Characteristics of each sensor are shown in Table 1. These two different sensors were used to assess the impact of spatial resolution on the delineation of the features of interest. The overlap in the radiometric and temporal ranges of the two products allows for such a comparison. Top-of-atmosphere (TOA) reflectance products were used for both sensors. Bottom-of-atmosphere (BOA) or surface reflectance (SR) products with atmospheric corrections were also assessed but found to show no significant differences for the purposes of this analysis. While it has been shown that atmospheric correction results in a relative increase of vegetation indices and can introduce errors that vary depending on landcover class (Seong et al. 2020; Rech et al. 2023), this did not hinder the results here. TOA images were thus selected because an additional 21 months of imagery was available for the S2 sensor

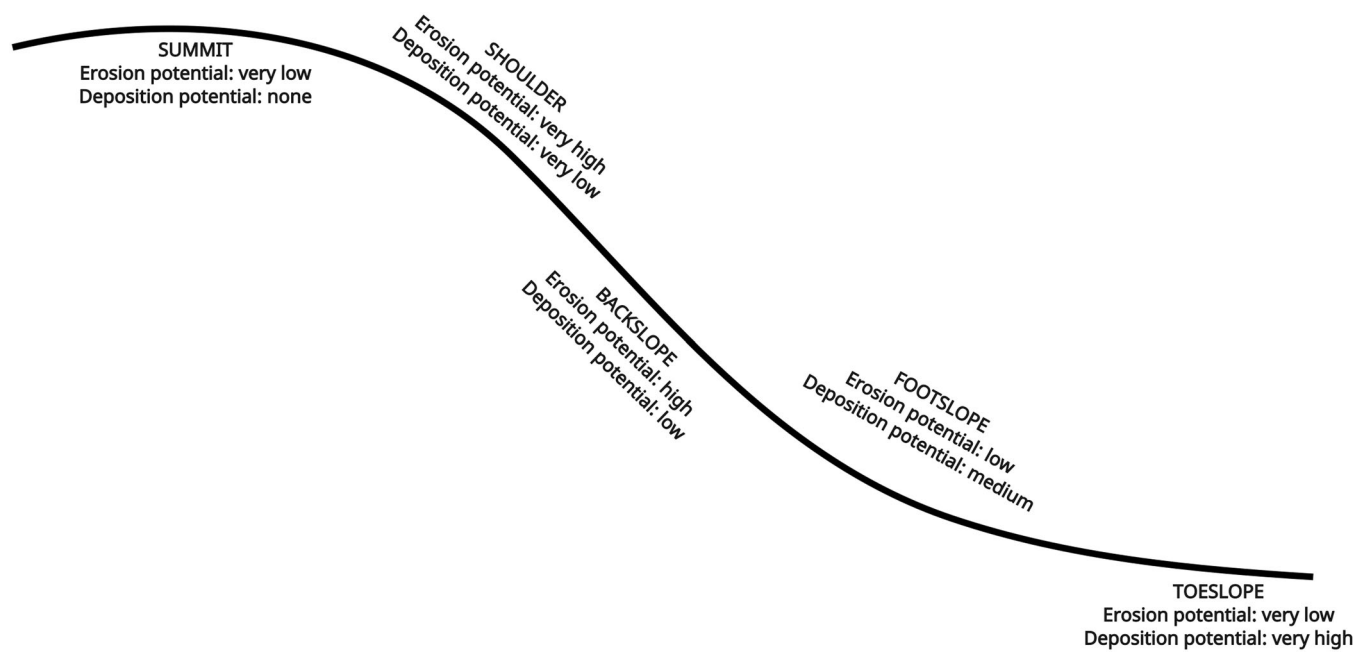


**FIGURE 4** | Model showing hillslope components and generalized erosion and deposition potential associated with each. Modified from Schaetzl (2013, Figure 3).

**TABLE 1** | Key characteristics of Sentinel-2 and Landsat-8 sensors.

	Sentinel-2	Landsat-8
Spatial resolution	10 m	30 m
Radiometric resolution (central wavelengths of optical bands)	B2: 492.4 nm (Blue) B3: 559.8 nm (Green) B4: 664.6 nm (Red) B8: 832.8 nm (NIR)	B2: 480 nm (Blue) B3: 560 nm (Green) B4: 655 nm (Red) B5: 865 nm (NIR)
Temporal resolution	5 days (2–3 at mid-latitude)	16 days
Launch date	June 2015	February 2013
Number of unique images used in multi-temporal composites	662	285

(available from June 2015, as opposed to SR images available only from March 2017).

A mean pixel-wise reducer was used to produce the multi-temporal composite after cloud masking (using the bitmask cloud bands). The mean reducer produced a more homogenous image than the median, resulting in more within-field noise and complicating the delineation of contrasts, particularly when dealing with the smaller image collections for subperiods, as outlined below.

To further enhance contrasts in the image composites, non-visible bands of the multi-spectral instruments were used to compute spectral indices. Vegetation indices are widely used to assess vegetation health, based on the increase in reflectance that occurs in the near-infrared part of the spectrum owing to the presence of leaf pigments in healthy vegetation (Jensen 2014, chap 11), with the Normalized Difference Vegetation Index (NDVI) being the most commonly applied. The Enhanced Vegetation Index (EVI), which corrects for some atmospheric and soil background effects, was initially used, following the protocol outlined by Orengo and Petrie (2017), but further trials indicated

that nearly identical results are obtained using NDVI. This may be because the EVI primarily offers improved sensitivity in areas of particularly high biomass (Jensen 2014, 393). Vegetation indices were calculated on the resulting multi-band mean image computed after the cloud masking described above.

Geophysical survey was also used to characterize intra-field variability at higher resolution and for a more direct assessment of subsurface properties. Frequency-domain electromagnetic (FDEM) survey was used in a multicoil configuration, which allows for simultaneous evaluation of electrical conductivity (EC) and magnetic susceptibility (MS) at different depths. The instrument used was the DualEM-21H (DualEM, Canada), equipped with a transmitting coil operating at 9 KHz and three pairs of receiving coils oriented horizontally coplanar (HCP pairs at 0.5, 1, and 2 m spacing) or perpendicular (PRP pairs at 0.6, 1.1, and 2.1 m spacing) to the transmitting coil. This renders so-called apparent values (ECa and MSa, respectively), which assume a homogenous subsurface. A mobile configuration was used, whereby the instrument is towed behind a quad bike equipped with a GPS and navigation unit. Survey transects with 2 m spacing were used, with an approximate 25 cm in-line

sampling density. After calibration of the raw data for temporal drift (Hanssens et al. 2021), interpolation to 50 cm resolution was undertaken. A 1D inversion procedure using EMagPy (McLachlan et al. 2021) was also used to investigate vertical variations in conductivity and examine differences between the apparent conductivities and modeled “true” distributions.

Limited invasive sampling using boreholes was also undertaken along several transects to record soil profiles and collect samples for further laboratory analysis. An Edelman auger (10 cm diameter) was used at select locations both inside and outside colluvial deposits (according to the existing soil mapping and results of the FDEM surveys). Soil descriptions were recorded for each borehole, and at least one bulk sample was taken from each recorded soil horizon. Samples were weighed and oven-dried for 24 h at 105°C to record gravimetric moisture content. The resistivity of the bulk sample was measured in the lab using a soil box and a resistivity meter with a four-electrode configuration (Miller 400D, M.C. Miller, USA). Texture analysis was then performed on select soil samples using the pipette method (Standard NF X31-107).

## 5 | Results

The classified landforms map based on the geomorphons method is shown in Figure 5. The depositional areas show where colluvial deposits are likely to accumulate, with the steep slopes indicating the most erosion-prone areas. Overlaying the mapped colluvial deposits from the existing soil mapping (Louis 1958, 1973) shows a high degree of correspondence (with areas of high erosion risk located immediately adjacent to indicated extents of colluvial deposits), following the typical model of catena development (Schaetzl 2013).

Figure 6 compares high-resolution orthophotos from different years for Area A, showing the widely varying contrasts that the colluvial deposits and eroded areas present under different conditions. These differing contrasts are due to the environmental conditions at the time the photo was taken (soil moisture, vegetation cover, and phenological stage of crop). It appears that, under certain conditions, colluvial deposits tend to support greener (i.e., healthier) vegetation, and eroded areas between them appear as comparatively bare soil (lighter colored) (e.g., 2007, 2015, 2019, and 2022). While the latter phenomenon is logical and consistent with what has been observed elsewhere (Netopil et al. 2022), the association of vegetation health with colluvial deposits has been less well-established in the literature.

This relationship appears to be valid across large portions of the study area, but its year-to-year manifestation is very inconsistent. Under relatively bare (low biomass) conditions, for instance (e.g., 2021), areas of apparently bare soil (appearing brighter) are visible within certain colluvial deposits, with intervening eroded or transitional areas appearing darker. Examination of S2 scenes from approximately the same dates, however, shows that vegetation indices are still marginally higher in the colluvial deposits. In other photos (e.g., 2016), distinct (ephemeral) gullies are visible as narrow linear features within larger colluvial deposits, indicating further gully erosion

taking place within certain depositional areas. Where multiple crops at different phenological stages are present, contrasts are difficult to discern in certain areas (e.g., 2007, 2017). Lastly, there are also examples of photos where no contrast is visible despite uniform crop coverage (e.g., 1994). Figure 6 also includes EVI values extracted from S2 images of approximately the same date as each orthophoto (for images post-dating 2015) for areas inside (A) and outside (B) mapped colluvial deposits. Transects through a colluvial deposit are also shown to help illustrate the contrasts in vegetation health. While certain images (e.g., 2007, 2015, 2019, 2022) do appear to show a correspondence between healthier vegetation and colluvial deposits, these examples show that the relationship is highly variable.

As previously noted, multi-temporal composites provide a way of overcoming varying conditions related to seasonality and land use. Figure 7 shows a mean-reduced composite of EVI values for the S2 data set with darker-colored zones representing higher EVI values.

There appears to be a correspondence between certain areas with higher EVI values and the colluvial deposits on the existing soil mapping, as highlighted in the insets of Figure 7. This relationship is highly dependent on land use, however, as seen in the various orthophotos in Figure 6. Greater detail can be seen in the EVI composite (Figure 7), with some additional areas that are not shown on the existing mapping. Comparing the EVI composite with the landform mapping, however, shows very good correspondence. Contrasts are quite subtle in terms of absolute values, as demonstrated in the sampled point locations and profiles in Figure 7. Demonstrating this correlation quantitatively across a large area is challenging due to the high inter-field variability of EVI values (influenced primarily by crop type and phenological stage), in addition to the soil classes and geomorphons, both being nominal data types. Nevertheless, there does appear to be a qualitative relationship.

Thus, colluvial deposits appear to show a tendency in this soil environment to support healthier vegetation, as was suggested by the examination of certain individual air photos above. The exact reasoning for this remains somewhat unclear but is perhaps due to a preferential moisture regime (i.e., more plant-available moisture), which could relate to texture differences (de Jong Van Lier et al. 2023) and increased organic matter in these areas (Schaetzl 2013, Figure 3; Lal 2020). Despite the visible presence of these patterns, attempts at segmentation of the Sentinel-2 data set, using K-means clustering proved unsuccessful, with the colluvial deposits failing to be extracted. Instead, the clustering algorithm identifies the individual fields as the major contrasts, highlighting the more significant inter-field variability. The contrasts between the colluvial deposits and the soil background are much subtler and thus obscured by these other larger variations.

The impact of spatial resolution is clear when comparing the results of the S2 EVI image with a Landsat-8 image over the same period (Figure 8). While some of the largest features (> 30 m dimension) are still vaguely present, there is a considerable reduction in visibility of within-field variability, with the major contrasts being those between fields. Given that many of

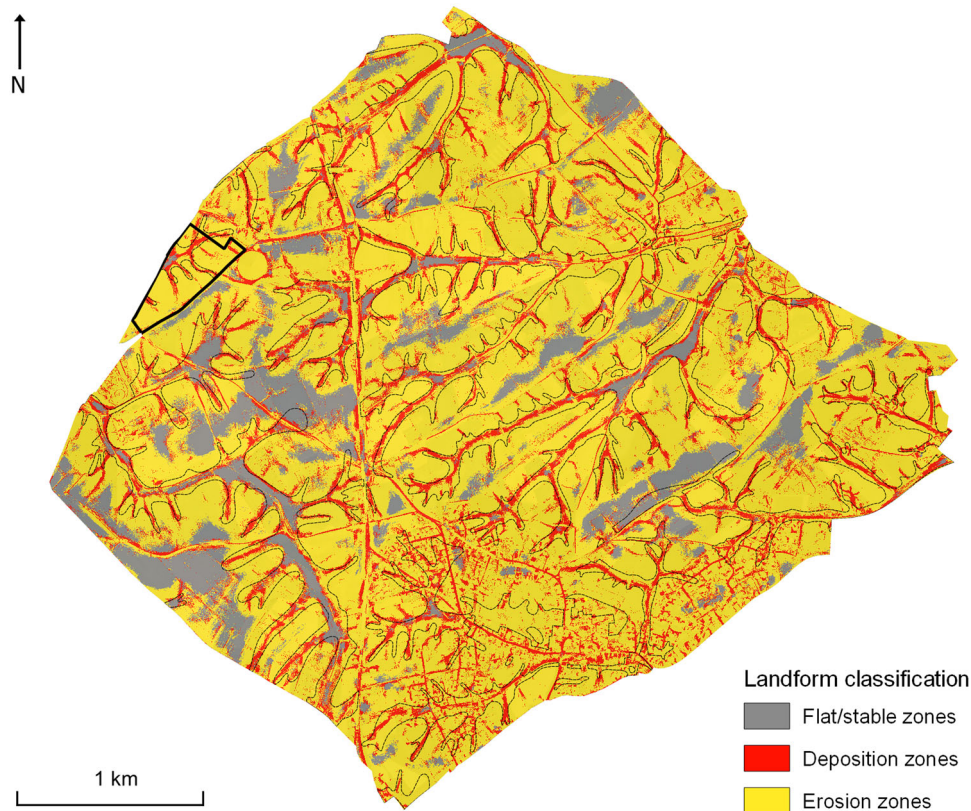


**FIGURE 5** | Terrain landforms classified using the geomorphons method for the entire study area. Dotted black lines indicate colluvial deposits mapped during mid-20th-century soil surveys. Area A is shown in solid black at the northwest edge.

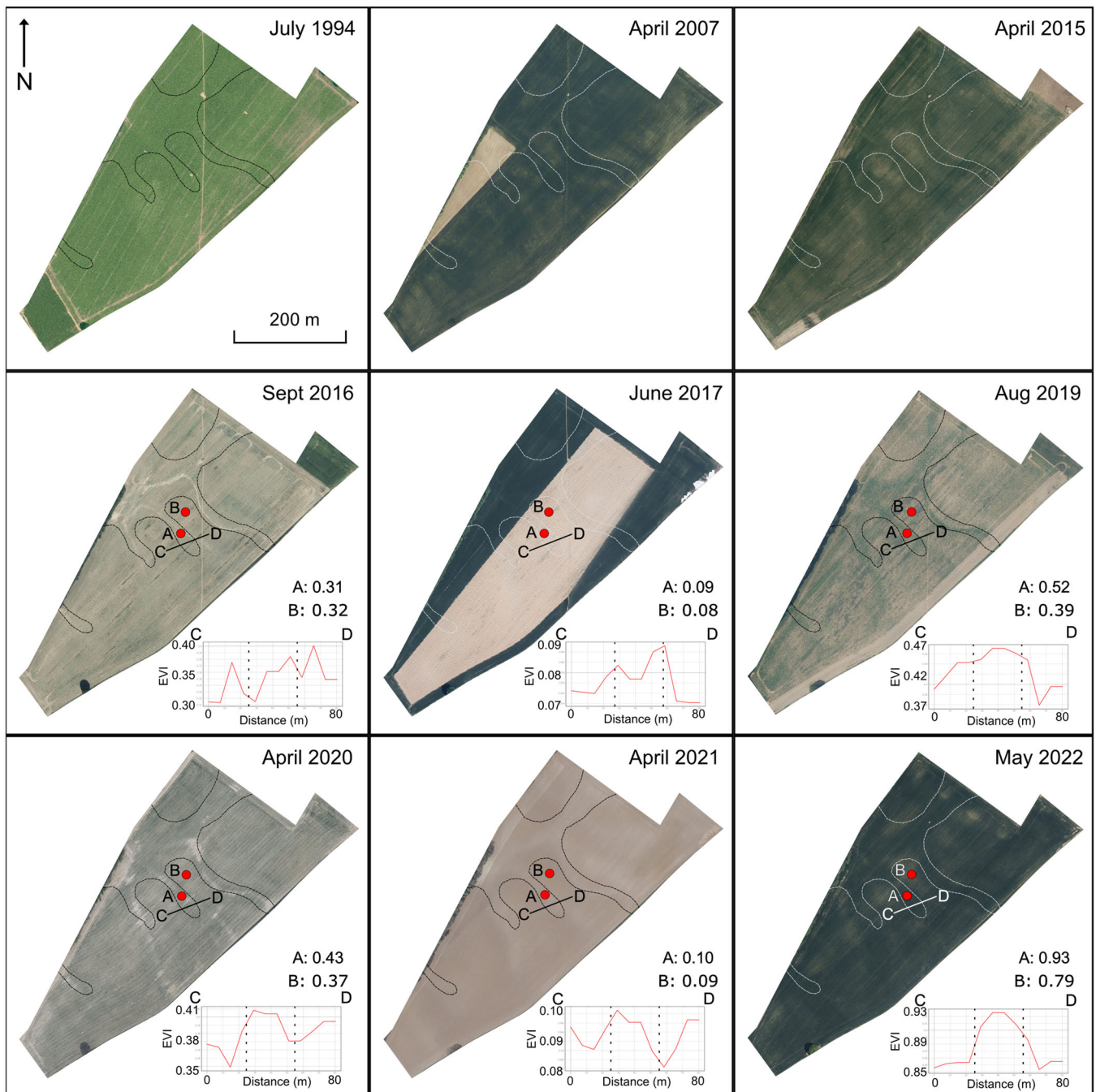
the mapped colluvial deposits have widths smaller than the Landsat spatial resolution (30 m), this is unsurprising. Area A serves as a good example of this, with all mapped deposits in this field having widths of less than 30 m. This suggests that further increasing the resolution of remote sensing datasets beyond the 10 m of the S2 datasets could yield additional insight, and indeed, this is the case with the orthophotos noted above.

Turning to the geophysical data, a map of FDEM apparent ECa for coil pair HCP1 is shown in Figure 9 for the entire study area. The lighter colored zones represent areas of lower conductivity (higher resistivity). There appears to be a pattern whereby some of the linear resistive zones correspond to colluvial deposits mapped on the existing soil surveys, although with more local variability (given the much higher sampling resolution). Again, it is difficult to demonstrate this quantitatively, given the nominal data types involved. Conductivity contrasts observed in the colluvial zones are likely primarily due to the smaller contribution of the clay-rich (i.e., high-conductivity) Bt horizon to the cumulative measured volume in these areas, as it is more deeply buried beneath recently eroded material. At the same time, the colluvial deposits themselves are characterized by coarser textures than the Bt horizon found at the same depth outside these zones (see below). Figure 10 shows ECa for each coil pair for Area A; the relative contrasts remain quite consistent across the different coil pairs, although the overall values increase due to the increasing influence of the Bt horizon in the deeper coil pairs. Inverted depth slices for Area A (at depths of 0.3 and 1 m, corresponding approximately to the bottom of the

plowzone and the Bt/colluvium interface) also show very similar patterning (Figure 11), indicating that the ECa maps are quite robust for predicting areas of colluvial deposition. Furthermore, a K-means clustering for the ECa data shows that these features can be extracted very effectively compared to the remote sensing data examined above (Figure 12).

An advantage of the FDEM method is that magnetic susceptibility (MSa) data is simultaneously gathered by processing the in-phase component of the received signal. This data is not considered here because it does not seem to offer additional insights beyond the ECa data for delineating colluvial deposits. In certain areas, however, colluvial deposits do appear to correspond to areas of enhanced MSa (see Area A example below). This may relate to the accumulation of organic matter and buried A-horizons in these areas, which are typically associated with higher magnetic susceptibility (Le Borgne 1955; Fassbinder 2015; Shirzaditabar and Heck 2022). These insights suggest intriguing potential applications for magnetic data in the mapping of erosion processes, which has been a little-explored avenue to date in the literature. The EC data, however, does appear to be a more robust proxy in this case and has other advantages, including a higher instrument signal-noise ratio and more straightforward inversion (the MSa data being uncalibrated).

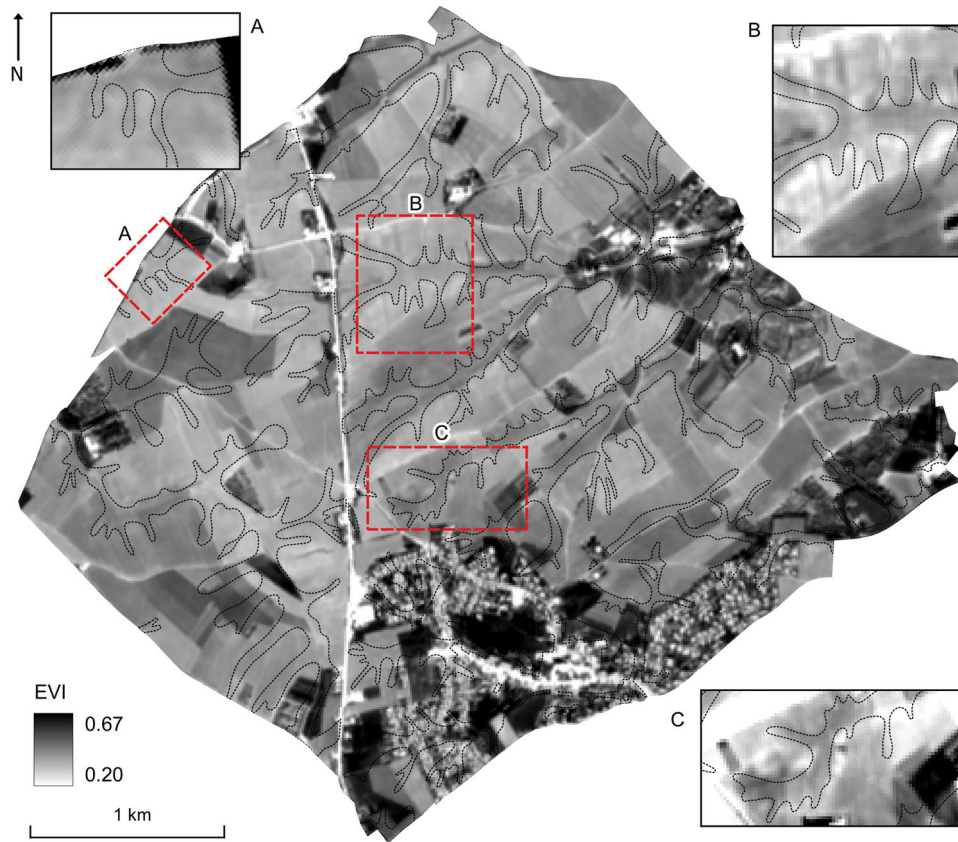
Figure 13 summarizes the terrain modeling, remote sensing, and geophysical datasets for Area A and shows the location of the reference transect along which invasive sampling was undertaken. Sample profiles are also shown for each data set to emphasize the contrasts that allow for the identification of the



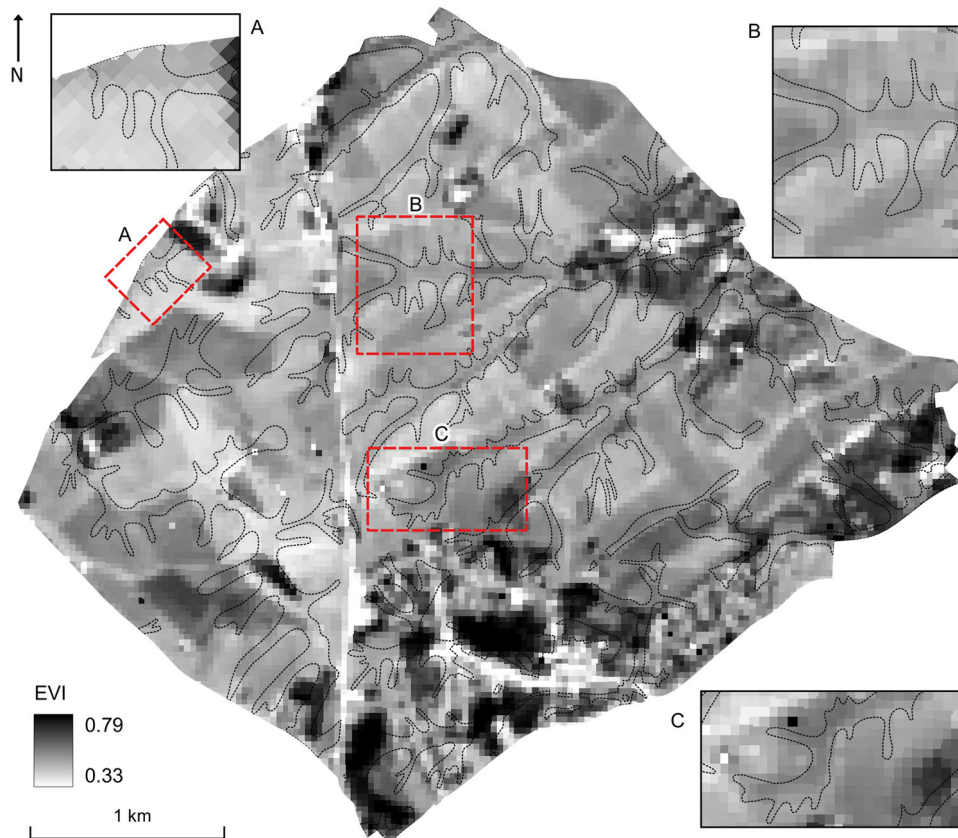
**FIGURE 6** | Orthophotos from various years showing varying contrasts of colluvial deposits. The point values shown for locations A and B are EVI values extracted from Sentinel-2 images of approximately the same date. Note that Sentinel-2 images are only available as of June 2015. The profiles shown along transect C-D also demonstrate the EVI contrasts, with the dotted lines demarcating the colluvial zones as mapped on soil surveys. Note how the EVI contrasts are quite robust for 2019, 2020, and 2022 but erratic for the other images.

colluvial deposit. To further explore the quantitative relationship between different datasets and complement the qualitative patterns that have been noted, a correlation between the EVI and ECa was calculated for the Area subset (after resampling to a common resolution and removing the extreme upper and lower 1% outliers). This yielded a correlation coefficient of  $-0.41$ , signifying a moderately negative relationship, which is consistent with the observed trends of colluvial deposits being associated with higher EVI and lower ECa values. The subtle nature of the contrast (between 5% and 10% in relative terms or about 3–4 mS/m and 0.02 EVI in absolute terms—see profiles

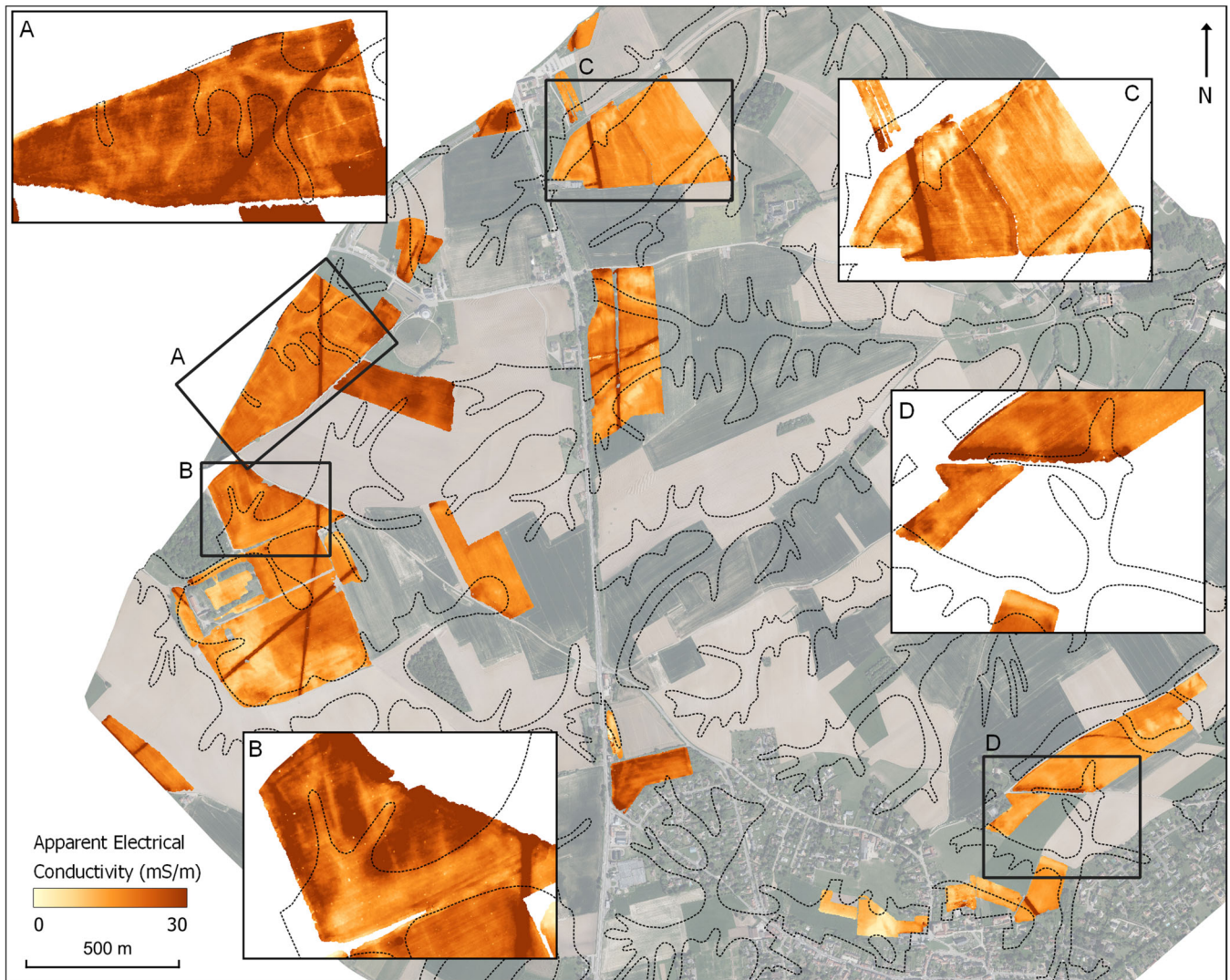
below) likely precludes a higher coefficient, with noise adding considerable uncertainty. Nonetheless, this quantitative relationship supports the qualitative observations. While the land-form classification from the geomorphon calculation and the soil classes from the soil mapping cannot be included in the correlation matrix (as nominal data types), they can be used as the basis for calculating zonal statistics on the quantitative data. Thus, colluvial zones are calculated as having mean ECa values of 21.6 (vs. 23.1 elsewhere or a 7% increase) and mean EVI values of 0.359 (vs. 0.343 elsewhere or a 4.5% increase), which further agrees with the trends noted above.



**FIGURE 7** | Mean composite of EVI values from Sentinel-2 data (662 images, June 2015–September 2023). The mapped colluvial deposits from the mid-20th century soil surveys are overlaid as dotted lines. Insets show certain areas in more detail where higher EVI values can be seen associated with the colluvial deposits.



**FIGURE 8** | Mean composite of EVI values from Landsat-8 data (285 images, June 2015–September 2023). Compare with Figure 7.



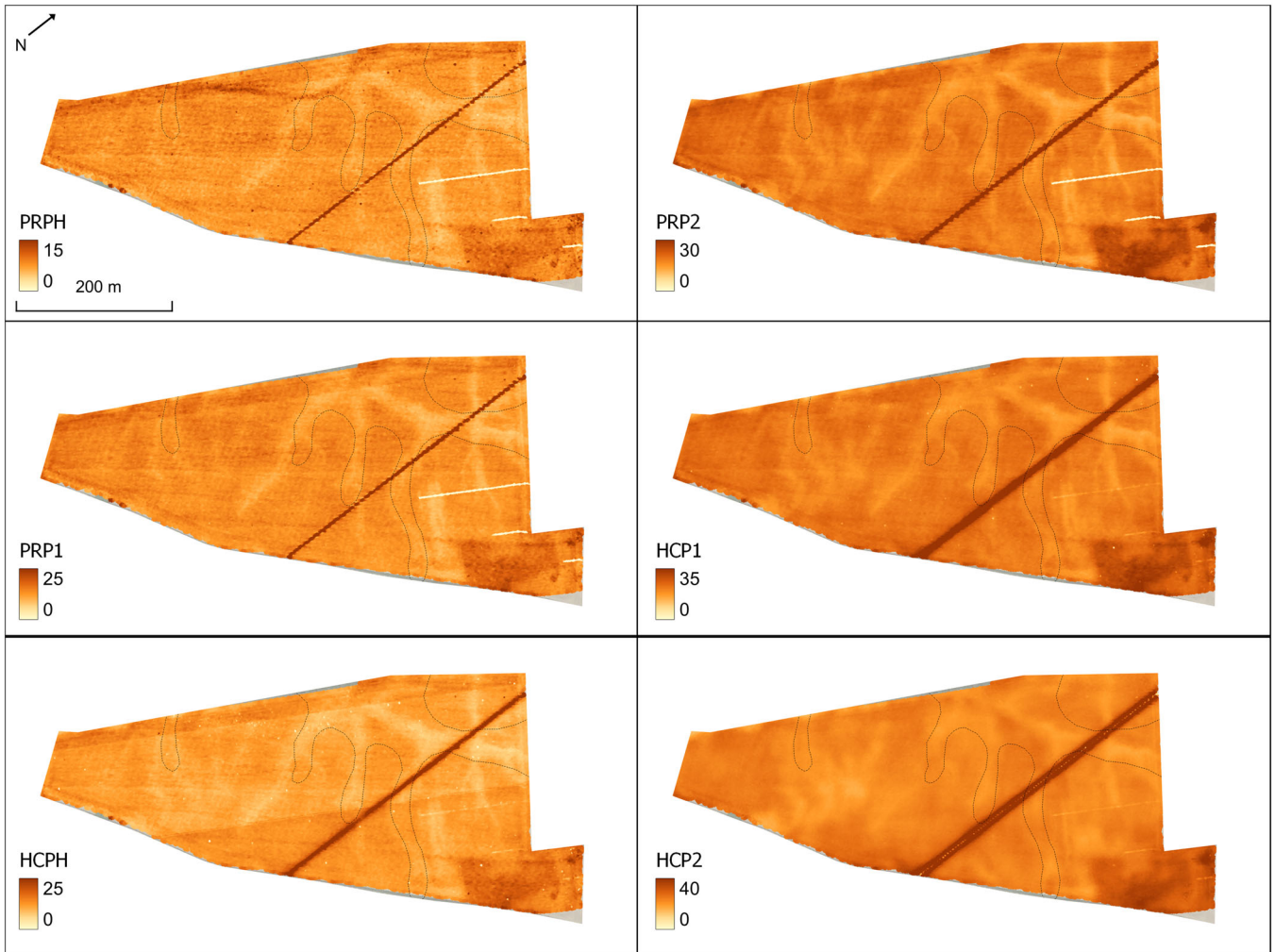
**FIGURE 9** | Apparent electrical conductivity data for coil pair HCP1. A total of 106 hectares of data was collected across the battlefield, as shown here. The mapped colluvial zones from the mid-20th century soil surveys are overlaid in dotted black lines. Insets highlight certain areas showing linear resistive contrasts that appear to correspond well to mapped colluvium (a smaller value range [0–20] is shown in these inset areas to highlight lower conductivity contrasts).

Figure 14 shows an inverted conductivity profile from the FDEM data set for a reference transect through a colluvial deposit in Area A. The deposit is visible in the lateral ECa data as an area of lower conductivity (about 5 mS/m or 20% lower than the adjacent areas, as shown in the sample profile in Figure 14), although it is not recorded as a colluvial deposit in the existing soil mapping. Terrain modeling indicates that a small portion of the transect crosses through a depositional area but that it is not as well-defined as other depositional areas in the parcel. It is also visible as an area of elevated EVI in the S2 data. The inverted profile shows a lower-conductivity zone in the center of the profile with a highly conductive layer at the same depth on either side.

Three boreholes were placed along the transect: one in the center of the low-conductivity feature and one on either side of it. These confirmed the variable depth of the Bt horizon, with the layer being found at a shallower depth outside the feature (at 30 cm depth, extending to approximately 1 m) and beneath

colluvial overburden in the center of the feature (appearing at 110 cm depth and extending to nearly 2 m) (Figure 15).

Laboratory (soil box) resistivity measurements (shown in Figure 15) confirmed the increased conductivity of the clayey Bt horizon and lower conductivity of the colluvium. The plowzone was found to be quite homogenous, with nearly identical conductivity across the three boreholes. Moisture content was variable, but the overall range is minimal and does not appear to be strongly correlated with conductivity or soil horizon. Results of soil texture analysis confirm that the increased clay content in the Bt horizon is responsible for the higher conductivity of this layer (Table 2). While all samples were classified as silty loam, the Bt samples have notably elevated clay content (between 4% and 5% higher than the overlying plowzone and colluvial deposits) and comparatively less fine sand (between one-third and half that of the colluvium). This represents a relative increase of about 30% in clay content and a decrease of about 60% in fine sand between the Bt and colluvium, indicating that texture clearly plays an important role in the



**FIGURE 10** | Apparent electrical conductivity for each coil pair for Area A with mapped colluvial deposits overlaid in dotted black. See Section 4 for the explanation of coil pair abbreviations. The depth indicated is the nominal depth of exploration for each coil pair, corresponding to the point above which 70% of the signal response is obtained. Note how the relative contrasts remain quite consistent between coil pairs, but the overall conductivity values increase.

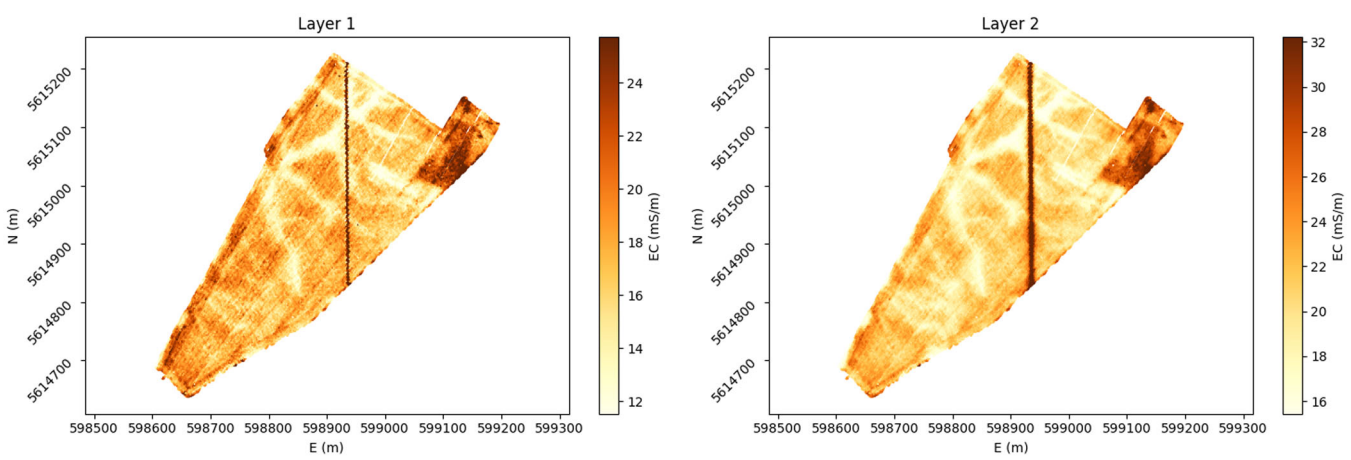


**FIGURE 11** | Inverted conductivity slices at depths of 30 cm (left) and 1 m (right). Note how the colluvial deposits are enhanced (compare with Figure 10).

formation of colluvial deposits. The increase in fine sands is consistent with the findings of other researchers, who report that soils with this texture are particularly susceptible to erosion (French 2016, 157).

Profiles of inverted conductivity for the borehole locations along this transect are shown in Figure 16. The different shapes allow for clear differentiation of the colluvial deposit: the boreholes outside the deposit have similar horizontal parabolic shapes,

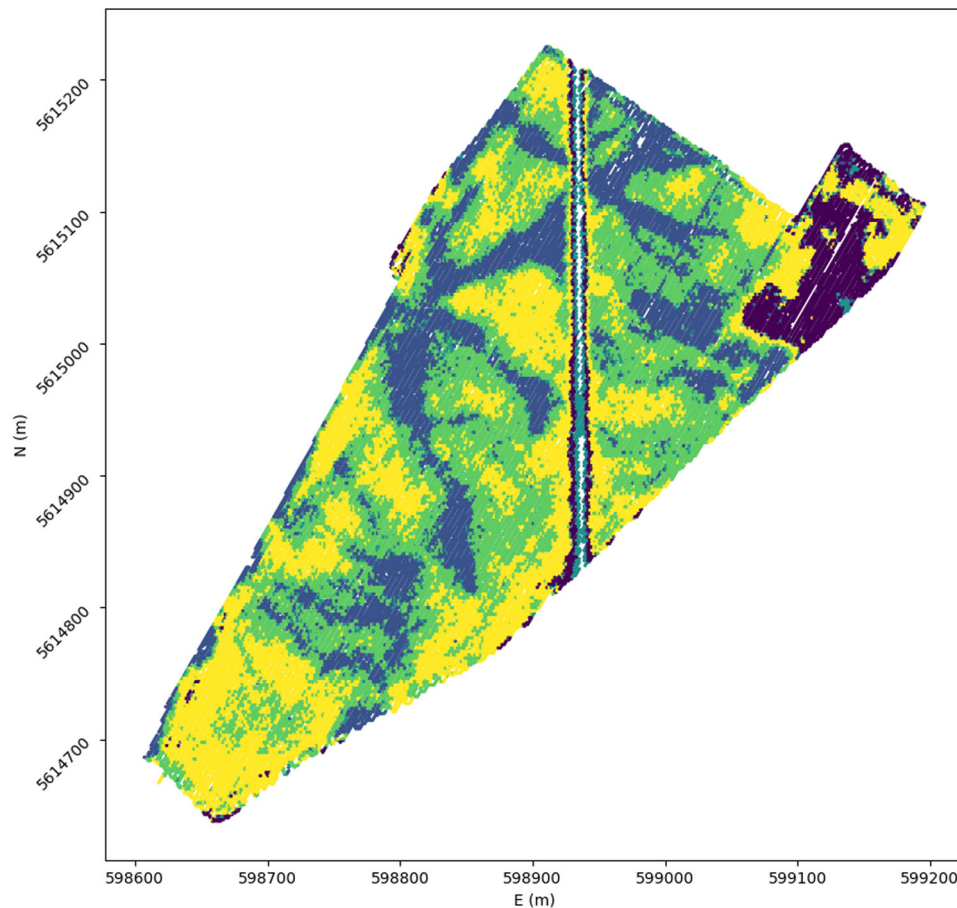


**FIGURE 12** | Results of k-means clustering of HCP1 apparent conductivity (five clusters). The color scale is arbitrary, with each color representing an individual cluster. Blue cluster corresponds to colluvial deposits.

reaching a maximum value at a depth that corresponds approximately to the Bt-C horizon transition, while the bore-hole inside the colluvial deposit has a less pronounced curve, a deeper maximum, and a more gradual decrease further down the profile. The decreasing conductivity at the base of each profile is due to the underlying sandy Tertiary substrate, also clearly reflected in the texture data (Table 2).

## 6 | Discussion

A review of the literature and field observations established water erosion as the main mechanism of soil movement and loss in the study area. Archaeological excavations at Waterloo have clearly established that colluvial deposits are significant in certain areas, with accumulation since the time of the battle often exceeding the effective search depth of commonly used methods (e.g., conventional induction balance metal detection, ca. 30 cm). This necessitates a better understanding of the distribution (both lateral and vertical extents) of colluvial deposits, allowing for adaptive archaeological prospection strategies. Commonly used methods for mapping and modeling soil erosion tend to operate at opposite ends of the scale spectrum. Thus, regional soil loss is typically modeled using equations with various environmental variables, and local variability is informed by point observations in traditional soil surveys. For

archaeological purposes, efficient mapping at high resolution is required (field or intra-field scale); this is demonstrated here using the measurement of proxy variables linked to soil properties for a more robust evaluation.

The preceding section shows how complementary methods can be integrated across different spatial scales to provide insight into the presence and extent of colluvial deposits in a loess soil environment. The remote sensing and terrain modeling approaches are most useful for rapid assessment at the landscape scale. Geophysical survey provides a higher-resolution field-scale perspective and a more detailed examination of the sub-surface than these methods allow. Targeted invasive sampling, combined with analysis of relevant soil properties, allows for a more robust understanding of sensor data and refinement of interpretations. The combination of these methods allows for bridging the gap noted above between discontinuous/labor-intensive field sampling and large-scale modeling approaches lacking the local resolution required for detailed mapping.

The terrain modeling using the geomorphons approach sought to define three main landforms: erosion-prone areas, depositional zones, and intermediary stable areas. It is suggested that using topography for defining erosional features is a robust approach in this case, given the homogeneity of other factors influencing erosion (rainfall erosivity, soil erodibility,

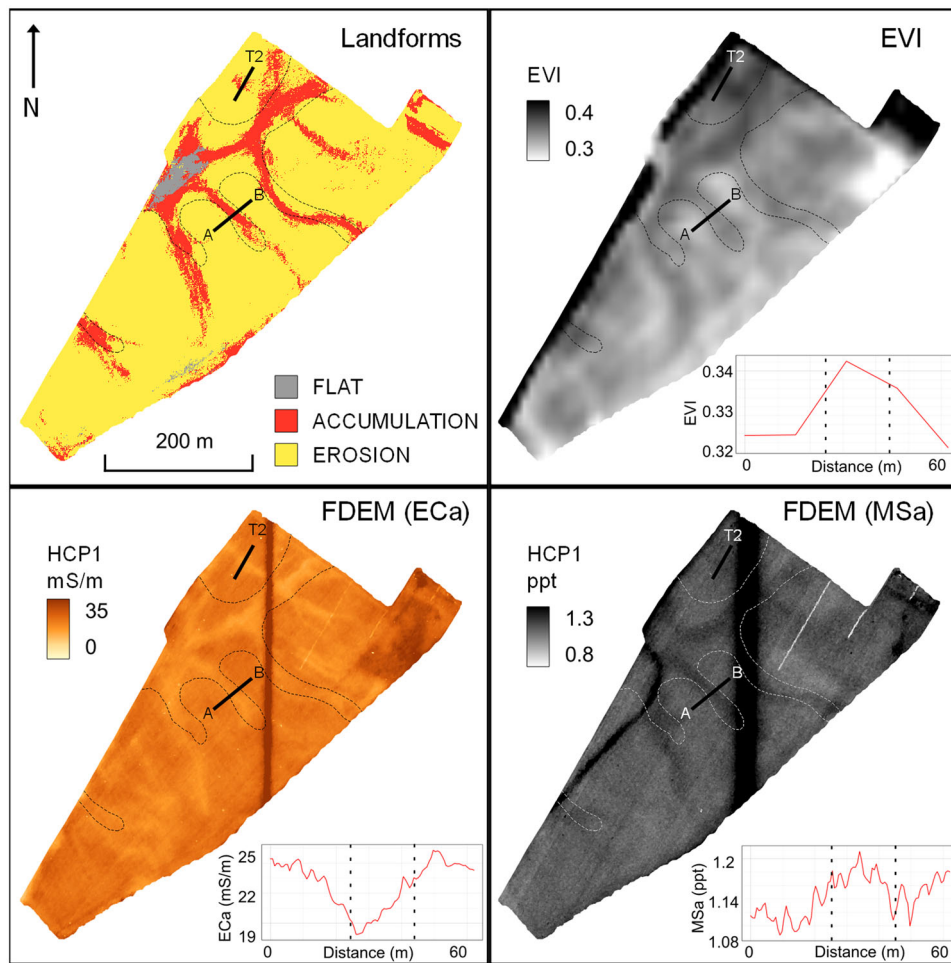


**FIGURE 13** | Terrain modeling, electrical conductivity, magnetic susceptibility, and Sentinel-2 EVI composite for Area A. Colluvial zones from the soil mapping are overlaid as dotted lines. The location of the reference transect described below is indicated by the solid line at the northern end of the parcel (T2). Values along another sample profile (marked A–B) are also shown to better illustrate the contrasts demarcating the colluvial deposits.

vegetation cover, and land use/support practices) at the scale of the study area. This approach, however, does not allow for the direct identification of colluvial deposits or even associated proxies, relying instead on terrain as a covariate (i.e., the association of certain landforms with soil erosion and deposition).

Recognizing the role of vegetation health as a proxy for the location of colluvial deposits in the study area (based on high-resolution orthophotos), vegetation indices were extracted from multi-temporal collections of multi-spectral remote sensing data. While many researchers have used the presence of higher indices (healthier vegetation) to infer a diminished risk of erosion (e.g., Ayalew et al. 2020) in modeling approaches, the association of vegetation and colluvial deposits has been less commonly employed; thus, it is an important proof of concept as presented here. The homogeneity of the soil environment in the study area allows for the recognition of subtle relevant contrasts in the remote sensing data. This complicates the (semi-) automated classification of the data set, however, given the relative weight of other contrasts (inter-field variability). Thus, the remote sensing approach is limited by land use constraints, which mask the more fine-grained variations of

interest. A multi-temporal approach for examining long-term trends provides one solution to this variability but also introduces a level of additional noise through the aggregation of different images under different conditions. Fine-tuning image selection and identifying ideal moments when contrasts are most evident (e.g., in periods of particularly high rain erosivity (Verstraeten et al. 2006) may assist in developing more robust composite datasets. This is particularly important with regard to higher-resolution imagery (< 5 m) with less frequent revisit times. While it remains difficult to calculate a straightforward quantitative correlation between colluvium and vegetation indices across a large area (due to the subtle contrasts, the presence of noise, and the nominal data types involved), the demonstrated correspondence and patterning between different datasets indicate the potential for the remote sensing approach.

The impact of spatial resolution was clearly demonstrated with the comparison of Landsat and Sentinel imagery, and the latter is still rather coarse for the identification of small features. Other remote sensing methods not examined here may also prove useful for identifying contrasts. In particular, sensors targeting soil moisture such as RADAR platforms (Jensen 2014, chap. 9) or possibly LiDAR intensity (Challis et al. 2011;

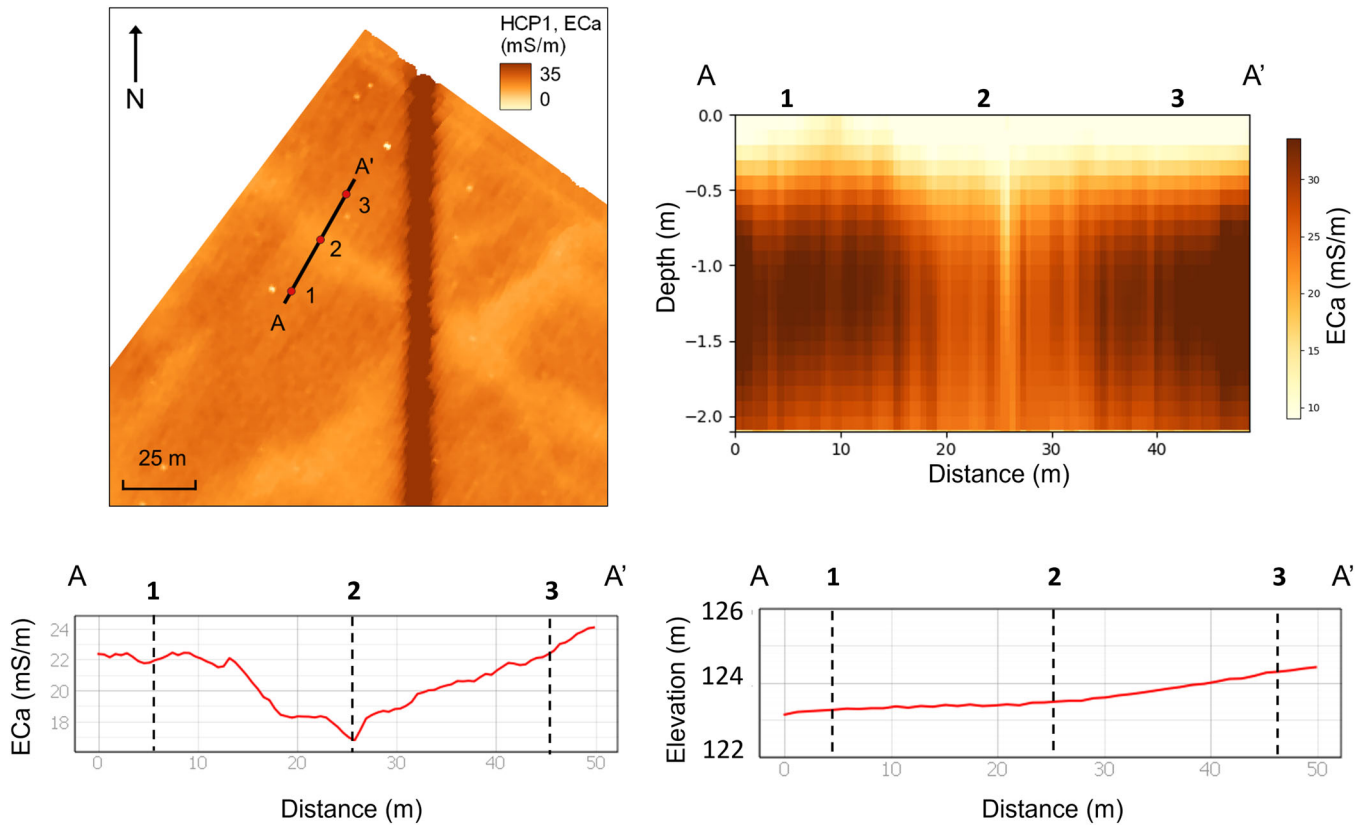


**FIGURE 14** | Reference transect in Area A. Location of transect and boreholes shown top left, inverted profile top right with borehole locations. ECa values (HCP1) and elevation across the transect shown on the bottom left and right, with borehole locations indicated.

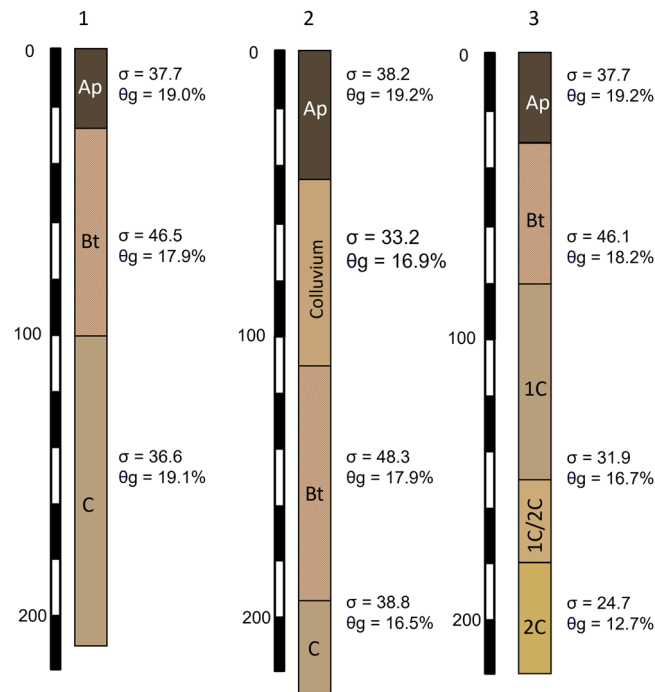


**FIGURE 15** | Soil profiles for boreholes along the transect, with conductivity ( $\sigma$ ) and gravimetric moisture ( $\theta_g$ ) of collected samples indicated.

Garroway et al. 2011) may prove effective, although these are also impacted by factors such as vegetation cover. The former has the advantage of high temporal resolution but typically lower spatial resolution, while the inverse is true for the latter.

Due to the homogeneity of the soil environment and the subtle nature of the contrasts, combined with the small scale of the features of interest, geophysical methods were employed for the higher-resolution mapping of soil properties. Measurement of (electrical) soil properties and their subsurface variation enabled relatively straightforward identification of colluvial deposits. This was accomplished largely by mapping soil texture variability, using conductivity as a proxy. Here, depth to the clay-rich Bt horizon is used as a proxy for the thickness of the colluvial overburden. Variations in soil texture, though still quite subtle, were clearly observable and confirmed by sampling and laboratory analyses. The 1D inversion of FDEM data provides further insight into the vertical variation of conductivity and, thus, the depths of soil horizons of interest. Inverted profiles can be examined in a qualitative manner to rapidly gain insight into the presence and extent of colluvial deposits. The inverted data correlates very well with field and laboratory observations of selected borehole samples, which is extremely promising for the interpretation of sensor data in this environment. Additional sampling could allow for the calibration of a quantitative model for predicting depths of relevant deposits (topsoil, colluvium, clay-rich Bt, and sandy substrate), a possibility that was not explored here.

A more detailed understanding of the distribution of colluvium at the site is archaeologically relevant for several reasons. First, it dictates the depth of archaeological deposits of interest and thus informs sampling strategies. Standard prospection methods may be ineffective in some cases, and techniques specifically aimed at deeply buried deposits may need to be

**TABLE 2** | Soil properties for samples from boreholes along Transect 2, Area A.

Borehole	Depth (cm)	Soil horizon	Organic matter (%)	Clay (%)	Fine silt (%)	Coarse silt (%)	Fine sand (%)	Coarse sand (%)	Moisture (%)	Conductivity (mS/m)
1	75	Bt	0.13	21.9	33.4	40.9	3.7	0.1	17.9	46.5
2	25	Ap	1.11	17.2	25.9	46.9	8.6	1.4	19.2	38.2
2	75	Colluvium	0.28	16.8	22.5	48.3	11.2	1.2	16.9	33.2
2	150	Bt	0.12	21.9	26.7	46.1	5.1	0.1	17.9	48.3
2	200	C	0.08	18.8	24.7	49.9	6.4	0.2	16.5	38.8
3	200	2C	0	12.7	14.3	65.6	7.2	0.2	12.7	24.7

considered, ranging from mechanical excavation to geoarchaeological sampling approaches (e.g., Missiaen et al. 2015). Geophysical survey should still be effective in most cases, although it may require some additional consideration of particular instrument choice and configuration (e.g. magnetometry in total-field rather than gradiometer mode) (Kvamme 2006; Crabb et al. 2022).

Second, for battlefield archaeology in particular, the depth of overburden has important implications as the effectiveness of relied-upon conventional metal detection may be severely hampered in certain areas. The assumption here is that objects originally deposited in certain areas will subsequently be covered over by eroded sediment and become undetectable. This is, however, not a straightforward assumption and is complicated by other factors, primarily the impact of plowing on the distribution of material in the topsoil (Yorston et al. 1990; Boismier 1997). There is also the strong possibility that downslope movement of some material would have occurred as part of the erosion process, as has been observed in many archaeological contexts (Smith 2001; Collins et al. 2016; McCoy 2021), although this should not be a universal assumption (James et al. 1994). In some cases, it has been documented that denser/heavier objects will be more susceptible to downslope movement, though this threshold is unclear, and the additional influence of fluvial erosion is a further complication (Rick 1976). For Waterloo specifically, and for battlefield contexts more generally, this is still poorly understood, but the detailed mapping of colluvial deposition as examined here provides an important starting point. The spatial integrity of artifact distributions is a particularly important consideration for battlefield archaeology; in many cases, artifact scatters are all that remains of a conflict site, and their spatial distribution thus has a great deal of interpretational value (Banks 2020). Identifying biases in the data set is thus of fundamental importance.

While the deep burial of archaeological deposits can be seen as a negative as far as the use of certain prospection methods, it is also a positive from the point of view of preservation (e.g., Bosquet et al. 2015). Thus, contexts sealed beneath colluvial overburden are less likely to be subject to plow damage, further erosion, bioturbation, etc. Conversely, those that existed in areas sensitive to erosion are more likely to have been destroyed. This is particularly relevant for the types of features related to battlefields, which tend to be very ephemeral.

A major limitation of the present study is that robust chronological information is missing, thereby preventing reconstruction of the sedimentation sequence in depositional areas of interest. Coarse relative dating is possible in cases where datable archaeological contexts are found beneath colluvial deposits, providing a *terminus post quem* for the overlying sediments. This is only possible, however, for in situ archaeological remains; using artifacts for the relative dating of colluvial deposits is less reliable given the possibility of mixed or inverted stratigraphy (French 2016, 166). In the case of Waterloo, the assumption that the majority of colluvial deposits are relatively recent (i.e., since the time of the battle) is probably valid. This is particularly related to the influence of mechanized plowing in the last half-century. It may be possible to gain further insight into historical rates of erosion through a change

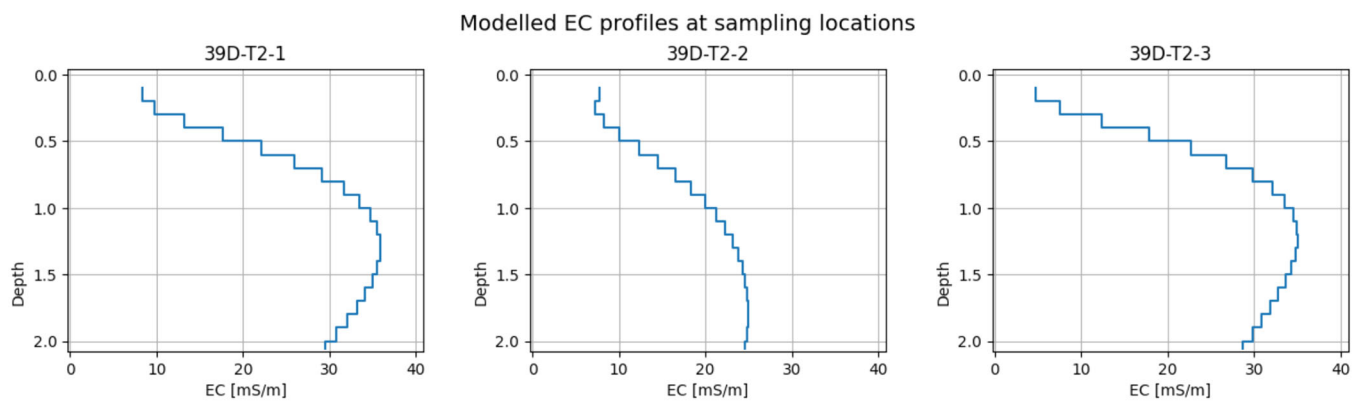


**FIGURE 16** | Inverted conductivity profiles for boreholes along reference transect.

detection approach, examining archive aerial photos to assess distributions of eroded areas (e.g., Jenčo et al. 2020; Netopil et al. 2022).

Aside from relative dating, there are several other methods that have the potential for a more refined understanding of the chronology of sedimentary sequences at Waterloo. One is optically stimulated luminescence (OSL), which has been widely applied to the dating of sediments in various contexts (Rhodes 2011), including colluvial sediments (Fuchs and Lang 2009; Lang 2015), and has a long history of archaeological applications (Duller 2008). The recent development of portable/rapid OSL readers has enabled the measurement of luminescence intensities on bulk unprocessed samples (e.g., soil profiles) (Sanderson and Murphy 2010; Munyikwa et al. 2021). While not allowing for the generation of an absolute age, this provides a proxy measurement for age, which can be used to examine variability in a profile and between sampling locations.

Another method that has shown great utility for dating post-World War 2 soil erosion is the analysis of fallout isotopes (cesium and plutonium) related to nuclear explosions (Wilkinson et al. 2006; Huisman et al. 2019). The displacement of soils over the past half-century has disrupted the original uniform distribution of these radioisotopes. Thus, in stable soil profiles, there is a decrease in concentration down the profile. Eroded areas show relatively lower concentrations, while depositional zones have higher concentrations. A related application is the use of phosphorus content, which relates to the introduction of chemical fertilizers in the early 20th century. Using the same principle as the isotopic tracers, it has been shown that the analysis of phosphorus levels in soil profiles can be used to estimate recent accumulation rates, although the method is less robust (Steege et al. 2000).

## 7 | Conclusion

Alongside impacts to other ecosystem services, soil erosion represents a critical ongoing threat to archaeological resources around the world, particularly in arable landscapes. In addition to monitoring and predicting future erosion rates for the purposes of site management, the reconstruction of sedimentary deposition at a site is a crucial step in the selection of appropriate sampling approaches and interpretation of archaeological data. Thus, the mapping of

areas of accumulating sediment (colluvium) is an important objective. While existing mapping products from regional soil surveys typically include some information on colluvial deposits, it is often desirable to gain a more detailed understanding of the lateral extent and depth of these deposits. We introduce a multi-scalar approach to mapping colluvial deposits, which integrates several noninvasive datasets: terrain derivatives to extract erosional and depositional landforms, optical remote sensing for determining vegetation health, and near-surface geophysics for characterizing soil properties. Informed by targeted invasive sampling and laboratory analysis of soil properties, this procedure allows for the detailed mapping and verification of the extent and depth of colluvial deposits.

The approach is demonstrated using a case study examining the Napoleonic battlefield of Waterloo, Belgium, situated in a loess environment particularly prone to soil erosion. With this framework in place, sampling approaches can be developed to target deposits in areas with increased overburden, which potentially have higher preservation of buried archaeological remains. This also allows for a better understanding of site formation processes, potential preservation biases, and interpretation of archaeological data via the association of artifacts and features with different sedimentary units. Important next steps include the development of a more robust chronological framework to relate colluvial deposits to archaeological layers of interest; at present, this is only known through relative dating via the association of sealed archaeological deposits with overlying sediments.

## Author Contributions

**Duncan Williams:** conceptualization, investigation, funding acquisition, writing – original draft, methodology, software, formal analysis, writing – review and editing; visualization, project administration. **Kate Welham:** conceptualization, funding acquisition, writing – review and editing, project administration, supervision. **Stuart Eve:** conceptualization, funding acquisition, writing – review and editing, supervision, project administration. **Philippe De Smedt:** conceptualization, methodology, writing – review and editing, software, data curation, formal analysis, supervision, visualization, resources, project administration.

## Acknowledgments

This work was supported in part by funding from the Social Sciences and Humanities Research Council (Canada), Waterloo Uncovered

(United Kingdom), Bournemouth University, and the Gray-Milne Bursary (British Geophysical Association).

## Data Availability Statement

Data that support the findings of this study are available from the corresponding author upon reasonable request.

## Endnotes

<sup>1</sup>Note that there is considerable variety in the published definitions of the term colluvium (see Miller and Juilleret 2016; Zádorová and Penížek 2018).

<sup>2</sup>Some limited exceptions include the use of ground-penetrating radar for identifying and mapping thickness of colluvial deposits, which has been successful in a variety of contexts (e.g., Aranha et al. 2002; Gerber et al. 2010).

## References

Ahmed, N., S. Masood, S. Ahmad, et al. 2019. "Soil Management for Better Crop Production and Sustainable Agriculture." In *Agronomic Crops*, edited by M. Hasanuzzaman, 47–71. Springer Singapore.

Ahrens, R. J. 2008. "Foreword." In *Digital Soil Mapping With Limited Data*, edited by A. E. Hartemink, A. B. McBratney, and M. de L. Mendonça-Santos, v–vi. Springer.

Aranha, P. R. A., C. H. R. R. Augustin, and F. G. Sobreira. 2002. "The Use of GPR for Characterizing Underground Weathered Profiles in the Sub-Humid Tropics." *Journal of Applied Geophysics* 49, no. 4: 195–210.

Ayalew, D. A., D. Deumlich, B. Šarapatka, and D. Doktor. 2020. "Quantifying the Sensitivity of NDVI-Based C Factor Estimation and Potential Soil Erosion Prediction Using Spaceborne Earth Observation Data." *Remote Sensing* 12, no. 7: 1136.

Banks, I. 2020. "Conflict Archaeology." In *The Routledge Handbook of Global Historical Archaeology*, edited by C. E. Orser and A. Zarankin, 192–214. Routledge.

Boardman, J. 1998. "An Average Soil Erosion Rate for Europe: Myth or Reality?" *Journal of Soil and Water Conservation* 53, no. 1: 46–50.

Boardman, J. and Poesen, J., eds. 2006. *Soil Erosion in Europe*. Wiley.

Boettinger, J. L., R. D. Ramsey, J. M. Bodily, et al. 2008. "Landsat Spectral Data for Digital Soil Mapping." In *Digital Soil Mapping With Limited Data*, edited by A. E. Hartemink, A. McBratney, M. de L. Mendonça-Santos, 193–202. Springer Netherlands.

Boismier, W. A. 1997. *Modelling the Effects of Tillage Processes on Artefact Distribution in the Ploughzone: A Simulation Study of Tillage-Induced Pattern Formation*. Archaeopress.

Bosquet, D., C. Barton, S. Eve, et al. 2016. *Waterloo Uncovered July 2016 Excavation Campaign*. Waterloo Uncovered.

Bosquet, D., G. Yernaux, A. Fossion, and Y. Vanbrabant. 2015. *Le Soldat de Waterloo: Enquête archéologique au coeur du conflit*. Service public de Wallonie: Département du patrimoine.

Brandolini, F., T. C. Kinnaird, A. Srivastava, and S. Turner. 2023. "Modelling the Impact of Historic Landscape Change on Soil Erosion and Degradation." *Scientific Reports* 13, no. 1: 4949.

Brazier, R. 2013. "Hillslope Soil Erosion Modeling." In *Treatise on Geomorphology*, edited by J. F. Shroder, 135–146. Academic.

Broggi, C., J. A. Huisman, L. Weihermüller, M. Herbst, and H. Vereecken. 2021. "Added Value of Geophysics-Based Soil Mapping in Agro-Ecosystem Simulations." *Soil* 7, no. 1: 125–143.

Challis, K., C. Carey, M. Kinsey, and A. J. Howard. 2011. "Airborne Lidar Intensity and Geoarchaeological Prospection in River Valley Floors." *Archaeological Prospection* 18, no. 1: 1–13.

Collins, B. D., D. R. Bedford, S. C. Corbett, C. Cronkite-Ratcliff, and H. C. Fairley. 2016. "Relations Between Rainfall–Runoff-Induced Erosion and Aeolian Deposition at Archaeological Sites in a Semi-Arid Dam-Controlled River Corridor." *Earth Surface Processes and Landforms* 41, no. 7: 899–917.

Connor, M., and D. D. Scott. 1998. "Metal Detector Use in Archaeology: An Introduction." *Historical Archaeology* 32, no. 4: 76–85.

Crabb, N., C. Carey, A. J. Howard, R. Jackson, N. Burnside, and M. Brolly. 2022. "Modelling Geoarchaeological Resources in Temperate Alluvial Environments: The Capability of Higher Resolution Satellite Remote Sensing Techniques." *Journal of Archaeological Science* 141: 105576.

Dawson, T., J. Hambly, A. Kelley, W. Lees, and S. Miller. 2020. "Coastal Heritage, Global Climate Change, Public Engagement, and Citizen Science." *Proceedings of the National Academy of Sciences United States of America* 117, no. 15: 8280–8286.

Domlija, P., S. Bernat Gazibara, Ž. Mihalić, and S. Arbanas. 2019. "Identification and Mapping of Soil Erosion Processes Using the Visual Interpretation of LiDAR Imagery." *ISPRS International Journal of Geo-Information* 8, no. 10: 438.

Dondeyne, S., L. Vanierschot, R. Langohr, E. Van Ranst, and J. Deckers. 2014. *The Soil Map of the Flemish Region Converted to the 3rd Edition of the World Reference Base for Soil Resources*. Vlaamse Overheid.

Duller, G. A. T. 2008. *Luminescence Dating: Guidelines on Using Luminescence Dating in Archaeology*. English Heritage.

Evans, M., S. Eve, V. Haverkate-Emmerson, T. Pollard, E. Steinberg, and D. Ulke. 2019. "Waterloo Uncovered: From Discoveries in Conflict Archaeology to Military Veteran Collaboration and Recovery on One of the World's Most Famous Battlefields." In *Historic Landscapes and Mental Well-Being*, edited by T. Darvill, 253–265. Archaeopress Publishing Ltd.

Eve, S., and T. Pollard. 2020. "From the Killing Ground: Digital Approaches to Conflict Archaeology—A Case Study From Waterloo." *Digital War* 1, no. 1–3: 144–158.

FAO. 2019. *Global Symposium on Soil Erosion: Outcome Document*. Food and Agriculture Organization of the United Nations.

Fassbinder, J. W. E. 2015. "Seeing Beneath the Farmland, Steppe and Desert Soil: Magnetic Prospecting and Soil Magnetism." *Journal of Archaeological Science* 56: 85–95.

French, C., H. Lewis, M. J. Allen, et al. 2007. "The Holocene History of the Upper Allen River Valley: Variation at the Sub-regional Scale." In *Prehistoric Landscape Development and Human Impact in the Upper Allen Valley, Cranborne Chase, Dorset*, edited by C. French, H. Lewis, M. J. Allen, M. Green, R. Scaife, J. Gardiner, 21–65. McDonald Institute for Archaeological Research; Distributed USA, David Brown Company.

French, C. A. I. 2016. "Colluvial Settings." In *Encyclopedia of Geoarchaeology*, edited by A. S. Gilbert, 157–170. Springer.

Froehlicher, L., D. Schwartz, D. Ertlen, and M. Trautmann. 2016. "Hedges, Colluvium and Lynchets Along a Reference Toposequence (Habsheim, Alsace, France): History of Erosion in a Loess Area." *Quaternaire* 27, no. 2: 173–185.

Fuchs, M., and A. Lang. 2009. "Luminescence Dating of Hillslope Deposits—A Review." *Geomorphology* 109, no. 1–2: 17–26.

Garré, S., G. Blanchy, D. Caterina, P. De Smedt, A. Romero-Ruiz, and N. Simon. 2023. "Geophysical Methods for Soil Applications." In *Encyclopedia of Soils in the Environment*, 444–458. Elsevier.

Garroway, K., C. Hopkinson, and R. Jamieson. 2011. "Surface Moisture and Vegetation Influences on Lidar Intensity Data in an Agricultural Watershed." *Canadian Journal of Remote Sensing* 37, no. 3: 275–284.

Gerber, R., P. Felix-Henningsen, T. Behrens, and T. Scholten. 2010. "Applicability of Ground-Penetrating Radar as a Tool for Non-destructive Soil-Depth Mapping on Pleistocene Periglacial Slope Deposits." *Journal of Plant Nutrition and Soil Science* 173, no. 2: 173–184.

- Gholizadeh, A., D. Žizala, M. Saberioon, and L. Borůvka. 2018. "Soil Organic Carbon and Texture Retrieving and Mapping Using Proximal, Airborne and Sentinel-2 Spectral Imaging." *Remote Sensing of Environment* 218: 89–103.
- Goovaerts, P. 2016. "Sample Support." In *Wiley StatsRef: Statistics Reference Online*, edited by R. S. Kenett, N. T. Longford, W. W. Piegorisch, and F. Ruggeri, 1–8. Wiley.
- Gorelick, N., M. Hancher, M. Dixon, S. Ilyushchenko, D. Thau, and R. Moore. 2017. "Google Earth Engine: Planetary-Scale Geospatial Analysis for Everyone." *Remote Sensing of Environment* 202: 18–27.
- Groß, J., N. Gentsch, J. Boy, et al. 2023. "Influence of Small-Scale Spatial Variability of Soil Properties on Yield Formation of Winter Wheat." *Plant and Soil* 493, no. 1–2: 79–97.
- Haesaerts, P., F. Damblon, N. Gerasimenko, P. Spagna, and S. Pirson. 2016. "The Late Pleistocene Loess-Palaeosol Sequence of Middle Belgium." *Quaternary International* 411: 25–43.
- Hanssens, D., W. Waegeman, Y. Declercq, H. Dierckx, H. Verschelde, and P. De Smedt. 2021. "High-Resolution Surveying With Small-Loop Frequency Domain Electromagnetic Systems: Efficient Survey Design and Adaptive Processing." *IEEE Geoscience and Remote Sensing Magazine* 9, no. 1: 167–183.
- Henkner, J., J. Ahlrichs, S. Downey, et al. 2018. "Archaeopedological Analysis of Colluvial Deposits in Favourable and Unfavourable Areas: Reconstruction of Land Use Dynamics in SW Germany." *Royal Society Open Science* 5, no. 5: 171624.
- Hill, J. B. 2004. "Land Use and an Archaeological Perspective on Socio-Natural Studies in the Wadi Al-Hasa, West-Central Jordan." *American Antiquity* 69, no. 3: 389–412.
- Hills, G. A. 1950. *The Use of Aerial Photography in Mapping Soil Sites*. Research Division, Ontario Department of Lands and Forests.
- Houthuys, R. 2011. "A Sedimentary Model of the Brussels Sands, Eocene, Belgium." *Geologica Belgica* 14, no. 1–2: 55–74.
- Huisman, H., J. W. De Kort, M. E. Ketterer, et al. 2019. "Erosion of Archaeological Sites: Quantifying the Threat Using Optically Stimulated Luminescence and Fallout Isotopes." *Geoarchaeology* 34, no. 4: 478–494.
- James, P. A., C. B. Mee, and G. J. Taylor. 1994. "Soil Erosion and the Archaeological Landscape of Methana, Greece." *Journal of Field Archaeology* 21, no. 4: 395–416.
- Jasiewicz, J., and T. F. Stepinski. 2013. "Geomorphons—A Pattern Recognition Approach to Classification and Mapping of Landforms." *Geomorphology* 182: 147–156.
- Jenčo, M., E. Fulajtár, H. Bobáľová, et al. 2020. "Mapping Soil Degradation on Arable Land With Aerial Photography and Erosion Models, Case Study From Danube Lowland, Slovakia." *Remote Sensing* 12, no. 24: 4047.
- Jensen, J. R. 2014. *Remote Sensing of the Environment: An Earth Resource Perspective*. Pearson.
- de Jong Van Lier, Q., S. D. Logsdon, E. A. R. Pinheiro, and P. I. Gubiani. 2023. "Plant Available Water." In *Encyclopedia of Soils in the Environment*, edited by D. Hillel, 509–515. Elsevier.
- Kappler, C., K. Kaiser, P. Tanski, et al. 2018. "Stratigraphy and Age of Colluvial Deposits Indicating Late Holocene Soil Erosion in North-eastern Germany." *Catena* 170: 224–245.
- Kvamme, K. L. 2006. "Magnetometry: Nature's Gift to Archaeology." In *Remote Sensing in Archaeology: An Explicitly North American Perspective*, edited by J. K. Johnson, 205–233. University of Alabama Press.
- Laga, P., S. Louwye, and S. Geets. 2002. "Guide to a Revised Lithostratigraphic Scale of Belgium." *Geologica Belgica* 4, no. 1/2: 135–152.
- Lal, R. 2020. "Soil Organic Matter and Water Retention." *Agronomy Journal* 112, no. 5: 3265–3277.
- Lang, A. 2015. "Luminescence, Colluvial Sediments." In *Encyclopedia of Scientific Dating Methods*, edited by W. J. Rink, J. W. Thompson, L. M. Heaman, A. J. T. Jull, and J. B. Paces, 490–492. Springer.
- Layzell, A. L., and R. D. Mandel. 2019. "Using Soil Survey Data as a Predictive Tool for Locating Deeply Buried Archaeological Deposits in Stream Valleys of the Midwest, United States." *Geoarchaeology* 34, no. 1: 80–99.
- Le Borgne, E. 1955. "Susceptibilité magnetique anormale du sol superficial." *Annales de Géophysique* 11: 399–419.
- Lehmkuhl, F., J. J. Nett, S. Pötter, et al. 2021. "Loess Landscapes of Europe—Mapping, Geomorphology, and Zonal Differentiation." *Earth-Science Reviews* 215: 103496.
- Liao, K., S. Xu, J. Wu, and Q. Zhu. 2013. "Spatial Estimation of Surface Soil Texture Using Remote Sensing Data." *Soil Science and Plant Nutrition* 59, no. 4: 488–500.
- Louis, A., 1958. *Texte explicatif de la planchette de Waterloo 116W*. l'Institut pour l'encouragement de la Recherche Scientifique dans l'Industrie et l'Agriculture. No. 116W.
- Louis, A., 1973. *Texte explicatif de la planchette de La Hulpe 116E*. l'Institut pour l'encouragement de la Recherche Scientifique dans l'Industrie et l'Agriculture. No. 116E.
- McCoy, C. 2021. "Colluvial Deposition of Anthropogenic Soils at the Ripley Site, Ripley, New York." *North American Archaeologist* 42, no. 1: 45–65.
- McLachlan, P., G. Blanchy, and A. Binley. 2021. "EMagPy: Open-Source Standalone Software for Processing, Forward Modeling and Inversion of Electromagnetic Induction Data." *Computers & Geosciences* 146: 104561.
- Meylemans, E., and J. Poesen. 2014. "The Archaeology of Erosion, the Erosion of Archaeology: An Introduction." In *The Archaeology of Erosion, the Erosion of Archaeology: Proceedings of the Brussels Conference, April 28-30 2008*, edited by E. Meylemans, J. Poesen, and I. I. Ven, 7–11. Flanders Heritage Agency.
- Meylemans, E., Poesen, J., and Ven, I. I., eds. 2014. *The Archaeology of Erosion, the Erosion of Archaeology: Proceedings of the Brussels Conference, April 28-30 2008*. Flanders Heritage Agency.
- Miller, B. A., and J. Juilleret. 2016. "Defining Colluvium and Alluvium: An Experiment to Discuss and Consolidate Perspectives." *Geophysical Research Abstracts* 18: EGU2016-17718.
- Missiaen, T., J. Verhegge, K. Heirman, and P. Crombé. 2015. "Potential of Cone Penetrating Testing for Mapping Deeply Buried Palaeolandscapes in the Context of Archaeological Surveys in Polder Areas." *Journal of Archaeological Science* 55: 174–187.
- Munykwa, K., T. C. Kinnaird, and D. C. W. Sanderson. 2021. "The Potential of Portable Luminescence Readers in Geomorphological Investigations: A Review." *Earth Surface Processes and Landforms* 46, no. 1: 131–150.
- Nachtergaele, J., J. Poesen, and G. Govers. 2002. "Ephemeral Gullies. A Spatial and Temporal Analysis of Their Characteristics, Importance and Prediction." *Belgeo* 2, no. 2: 159–182.
- Netopil, P., B. Šarapatka, D. A. Ayalew, and K. Drncová. 2022. "Multi-Temporal Analysis of Erosional Plots Using Aerial Images and Deep Soil Probes." *Physical Geography* 43, no. 6: 701–726.
- Van Oost, K., G. Govers, S. De Alba, and T. A. Quine. 2006. "Tillage Erosion: A Review of Controlling Factors and Implications for Soil Quality." *Progress in Physical Geography: Earth and Environment* 30, no. 4: 443–466.
- Van Oost, K., G. Govers, and P. Desmet. 2000. "Evaluating the Effects of Changes in Landscape Structure on Soil Erosion by Water and Tillage." *Landscape Ecology* 15, no. 6: 577–589.
- Orengo, H., and C. Petrie. 2017. "Large-Scale, Multi-Temporal Remote Sensing of Palaeo-River Networks: A Case Study From Northwest India

- and Its Implications for the Indus Civilisation." *Remote Sensing* 9, no. 7: 735–755.
- Penížek, V., T. Zádorová, R. Kodešová, and A. Vaněk. 2016. "Influence of Elevation Data Resolution on Spatial Prediction of Colluvial Soils in a Luvisol Region." *PLoS One* 11, no. 11: e0165699.
- Pennock, D. J. 2019. *Soil Erosion: The Greatest Challenge for Sustainable Soil Management*. Food and Agriculture Organization of the United Nations.
- Ray, R. G. 1960. *Aerial Photographs in Geologic Interpretation and Mapping*. United States Department of the Interior.
- Rech, B., J. H. Hess, S. J. de Souza Junior, and P. K. Uda. 2023. "Effects of Atmospheric Correction on NDVI Retrieved From Sentinel-2 Imagery Over Different Land Cover Classes." In *Presented at the Anais do XX Simpósio Brasileiro de Sensoriamento Remoto*. INPE.
- Rhodes, E. J. 2011. "Optically Stimulated Luminescence Dating of Sediments Over the Past 200,000 Years." *Annual Review of Earth and Planetary Sciences* 39, no. 1: 461–488.
- Rick, J. W. 1976. "Downslope Movement and Archaeological Intrasite Spatial Analysis." *American Antiquity* 41, no. 2: 133–144.
- Rommens, T., G. Verstraeten, I. Peeters, et al. 2007. "Reconstruction of Late-Holocene Slope and Dry Valley Sediment Dynamics in a Belgian Loess Environment." *Holocene* 17, no. 6: 777–788.
- Sanderson, D. C. W., and S. Murphy. 2010. "Using Simple Portable OSL Measurements and Laboratory Characterisation to Help Understand Complex and Heterogeneous Sediment Sequences for Luminescence Dating." *Quaternary Geochronology* 5, no. 2–3: 299–305.
- Schaetzl, R. 2013. "Catenas and Soils." In *Treatise on Geomorphology*, edited by J. F. Shroder, 145–158. Academic Press.
- Seong, N.-H., D. Jung, J. Kim, and K.-S. Han. 2020. "Evaluation of NDVI Estimation Considering Atmospheric and BRDF Correction Through Himawari-8/AHI." *Asia-Pacific Journal of Atmospheric Sciences* 56, no. 2: 265–274.
- Service public de Wallonie. 2005. *Carte des Principaux Types de Sols de Wallonie à 1/250000*, 1:250,000. Namur.
- Service public de Wallonie. 2015. *Relief de la Wallonie - Modèle Numérique de Terrain (MNT) 2013–2014*.
- Shirzaditabar, F., and R. J. Heck. 2022. "Characterization of Soil Magnetic Susceptibility: A Review of Fundamental Concepts, Instrumentation, and Applications." *Canadian Journal of Soil Science* 102, no. 2: 231–251.
- Smith, S. C. 2001. "Soil Erosion and Transport of Archaeological Sites and Artifacts on a Small Watershed in Northern New Mexico." Master's thesis, Colorado State University.
- Steege, A., G. Govers, L. Beuselinck, K. Van Oost, T. A. Quine, and A. Rombaut. 2000. "The Use of Phosphorus as a Tracer in Erosion/Sedimentation Studies." In *The Role of Erosion and Sediment Transport in Nutrient and Contaminant Transfer*, edited by M. Stone, 59–66. IAHS Publications.
- Vandaele, K., J. Poesen, J. R. Marques da Silva, and P. P. J. Desmet. 1996. "Rates and Predictability of Ephemeral Gully Erosion in Two Contrasting Environments." *Géomorphologie Relief Processus Environnement* 2, no. 2: 83–95.
- Vanwalleghe, T., H. R. Bork, J. Poesen, et al. 2006. "Prehistoric and Roman Gullying in the European Oess Belt: A Case Study From Central Belgium." *Holocene* 16, no. 3: 393–401.
- Vaudour, E., C. Gomez, Y. Fouad, and P. Lagacherie. 2019. "Sentinel-2 Image Capacities to Predict Common Topsoil Properties of Temperate and Mediterranean Agroecosystems." *Remote Sensing of Environment* 223: 21–33.
- Verstraeten, G., J. Poesen, G. Demarée, and C. Salles. 2006. "Long-Term (105 Years) Variability in Rain Erosivity as Derived From 10-min Rainfall Depth Data for Ukkel (Brussels, Belgium): Implications for Assessing Soil Erosion Rates." *Journal of Geophysical Research: Atmospheres* 111, no. D22: D22109.
- Verstraeten, G., J. Poesen, D. Goossens, et al. 2006. "Belgium." In *Soil Erosion in Europe*, edited by J. Boardman, J. Poesen, 387–411. Wiley.
- Vervust, S. 2016. "Deconstructing the Ferraris Maps (1770–1778): A Study of the Map Production Process and Its Implications for Geometric Accuracy." PhD thesis, Ghent University.
- Waterloo Uncovered. 2015. *An Archaeological Evaluation at Hougoumont Farm, Braine -l'Alleud 26th-29th April 2015*. Waterloo Uncovered.
- Weston, D. G. 2001. "Alluvium and Geophysical Prospection." *Archaeological Prospection* 8, no. 4: 265–272.
- Wilkinson, K., A. Tyler, D. Davidson, and I. Grieve. 2006. "Quantifying the Threat to Archaeological Sites From the Erosion of Cultivated Soil." *Antiquity* 80, no. 309: 658–670.
- Wischmeier, W. H., and D. D. Smith. 1978. *Predicting Rainfall Erosion Losses—A Guide to Conservation Planning*. U.S. Department of Agriculture. Agriculture Handbook.
- Yorston, R. M., V. L. Gaffney, and P. J. Reynolds. 1990. "Simulation of Artefact Movement Due to Cultivation." *Journal of Archaeological Science* 17, no. 1: 67–83.
- Zádorová, T., and V. Penížek. 2018. "Formation, Morphology and Classification of Colluvial Soils: A Review." *European Journal of Soil Science* 69, no. 4: 577–591.
- Zádorová, T., D. Žížala, V. Penížek, and Š. Čejková. 2014. "Relating Extent of Colluvial Soils to Topographic Derivatives and Soil Variables in a Luvisol Sub-Catchment, Central Bohemia, Czech Republic." *Soil and Water Research* 9, no. 2: 47–57.
- Žížala, D., A. Juřicová, T. Zádorová, K. Zelenková, and R. Minařík. 2019. "Mapping Soil Degradation Using Remote Sensing Data and Ancillary Data: South-East Moravia, Czech Republic." Supplement, *European Journal of Remote Sensing* 52, no. S1: 108–122.